Scalable Integrated Screening Tools for Cardiovascular Disease

by

Victoria Ouyang

B.S. Electrical Engineering and Computer Science, M.I.T., 2019

Submitted to the Department of Electrical Engineering and Computer Science
in partial fulfillment of the requirements for the degree of

Master of Engineering in Electrical Engineering and Computer Science

at the

MASSACHUSETTS INSTITUTE OF TECHNOLOGY

February 2020

Author . . . . . .
Department of Electrical Engineering and Computer Science
January 29, 2020

Certified by . . . . . .
Dr. Richard R. Fletcher
Research Scientist
Head, Mobile Technology Group
MIT D-Lab
Thesis Supervisor

Accepted by. . . . . .
Dr. Katrina LaCurts
Chair, Masters of Engineering Thesis Committee

Scalable Integrated Screening Tools for Cardiovascular Disease

by

Victoria Ouyang

Submitted to the Department of Electrical Engineering and Computer Science
on January 29, 2020, in partial fulfillment of the
requirements for the degree of
Master of Engineering in Electrical Engineering and Computer Science

Abstract

Cardiovascular disease (CVD) is the leading cause of mortality worldwide, accounting for more than 17.9 million deaths per year. Atherosclerosis, characterized by stiffening of the arteries, is the precursor to heart attacks and strokes, which cover 85% of all CVD mortalities. Since the disease is largely asymptomatic, a major challenge remains in screening for at-risk individuals. Existing screening tools primarily rely on questionnaires which do not account for ethnicity and require blood pressure and cholesterol readings. Thus, there is a crucial need for low-cost, non-invasive screening tools, especially in low-resource areas where people do not have access to routine clinical exams and blood tests.

To address these shortcomings, this thesis presents a scalable integrated CVD screening toolkit that is practical and can be deployed in a real-world setting. We have developed Android mobile apps and hardware capable of performing pulse wave analysis (PWA) and measuring pulse wave velocity (PWV) using PPG techniques. The analysis algorithms are configured to run on a custom server that is able to handle large amounts of medical data. In this thesis, I describe the PWA and PWV algorithms, the mobile applications associated with these measurements, and their integration with a custom server.

To validate these new algorithms, data was used from two separate clinical studies conducted by our group. For PWA, I analyzed PPG waveforms from young athletic people, young non-athletic people, old healthy people, and old CAD patients, which resulted in median PWA Scores of 3.51 (0.57), 3.19 (0.78), 1.98 (0.66), and 1.81 (0.5) respectively. From these results, the PWA tool demonstrated sufficient sensitivity to distinguish between the four different cardiovascular health classifications.

Based on a larger clinical study with 100 subjects at the Sengupta Hospital and Research Institute in Nagpur, India, I found that PWV in the central artery behaves differently from the PWV in peripheral muscular arteries. The study showed that central aortic PWV is a good indicator of atherosclerosis and coronary arterial disease. Using these results, I demonstrated that our machine learning algorithm is able to reliably distinguish healthy patients from non-healthy with an AUC of 0.83 (0.18).

Thesis Supervisor: Dr. Richard Fletcher
Title: Research Scientist
Head, Mobile Technology Group
MIT D-Lab

Acknowledgements

I would first like to thank my advisor, Dr. Rich Fletcher, for his dedicated support and guidance throughout this project. I am sincerely grateful for the opportunity to work on this impactful project, and for everything I learned about technology for medical applications.

I would also like to thank the doctors and nurses at the Sengupta Hospital and Research Institute who made the clinical studies in this project possible. In particular, Dr. Shantanu Sengupta and Dr. Kunda Mungulmare for their generous help and hospitality during my visits to India.

Thank you to the MIT Tata Center and staff for advice and seminars to guide the project, and supporting my travels to India. Diane Rigos and Chintan Vaishnav, who were invaluable mentors and taught me to think beyond just the technical aspects of the project.

Many thanks to John, Bo, and Shivani for their help and advice even after they graduated, and to the UROP students, Wilson, Julia, and Shwetark, who worked on this project with me.

To my friends who have supported and motivated me through all my years at MIT, I could not have done it without them.

Finally, a thank you to my family for their unconditional love, support, and encouragement.

Table of Contents

List of Figures

List of Tables

Chapter 1

Motivation and Thesis Scope

1.1 The Human Cardiovascular System

The human cardiovascular system consists of the heart and a closed system of blood vessels called arteries, veins, and capillaries. The heart is the center of the cardiovascular system. Each mechanical pump from the heart is controlled by a series of electrical impulses, and blood travels through the vascular system comprised of blood vessels and ultimately returns to the heart again. This sequence of events in which the heart undergoes a complete beat is known as the cardiac cycle. The two main parts of the cardiac cycle are the systole, when the heart contracts, and diastole, when the heart relaxes [1].

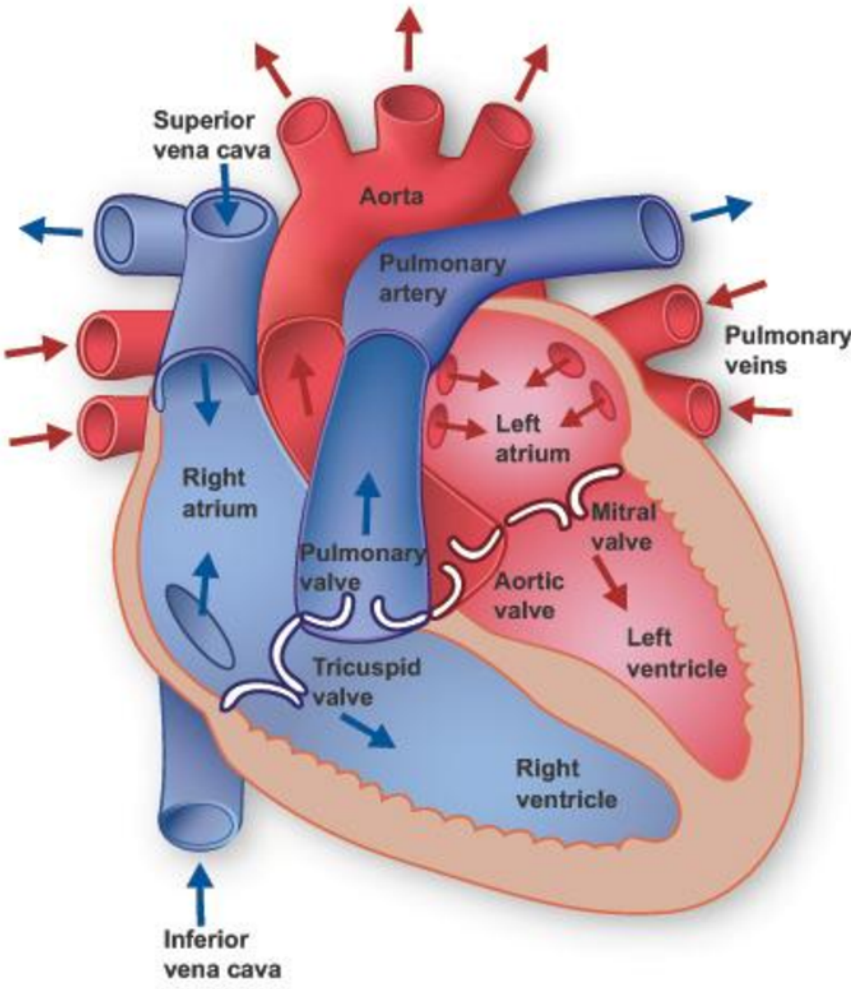

Figure 1.1: Anatomy of the Human Heart and Cardiac Cycle [2]

To understand the cardiac cycle in detail, we must first understand the structure of the heart. A typical human heart consists of four main chambers: the left ventricle, left atrium, right ventricle, and right atrium, as shown in Figure 1.1. Oxygenated blood flows out the left side of the heart, and deoxygenated blood flows into the right side of the heart [3]. The cardiac cycle can be organized into specific periods described as follows:

1. **First diastolic period:** Both the atria and the ventricles start in diastole at the beginning of the cycle. Deoxygenated blood fills into the right atrium, which is then passed into the right ventricle.

2. **First systolic period:** An electric impulse causes right atria to contract, which pumps blood from the right atrium into the right ventricle during the first diastolic period. A second contraction pumps the deoxygenated blood into the pulmonary artery and the lungs to replenish oxygen. Oxygenated blood is then returned to the heart through pulmonary veins.
3. **Second diastolic period:** Oxygenated blood fills into the left atrium, which is then passed into the left ventricle.
4. **Second systolic period:** An electric impulse triggers the left ventricle to contract and pump blood to the rest of the body.

Although the periods are termed first and second systolic and diastolic periods, these processes actually occur simultaneously on different sides of the heart during a single systolic and diastolic cycle [4].

1.2 What is Cardiovascular Disease?

Cardiovascular disease, or CVD, is a class of diseases that involve the heart or the blood vessels. They can be broadly classified as issues with the mechanical, electrical, or vascular components of the cardiovascular system, which all inevitably lead to problems of the entire system as a whole. Common classifications of CVDs are listed in Table 1.1. Of these classifications, vascular diseases are the most common among the general population [5].

Mechanical	Electrical	Vascular
Hypertension Cardiomyopathies Congenital Abnormalities Valvular Failures	Arrhythmias Conduction Issues	Atherosclerosis Aortic Dissections and Aneurysms

Table 1.1: Common Classifications of CVDs

1.3 The Burden of CVD

CVD is the leading cause of mortality worldwide, accounting for more than 17.9 million deaths per year according to the World Health Organization in 2019 [6]. This number is expected to grow to over 23.6 million by year 2030 [7]. In other words, 31% of all global deaths are due to CVD, and of these mortalities, 85% are due to heart attack and stroke. A third of these deaths occur prematurely in people under 70 years old [6]. In particular, over 80% of CVD mortalities occur in low and middle income countries due to lack of resources and awareness [7]. Figures 1.2 and 1.3 illustrate the burden of CVDs globally in 2017.

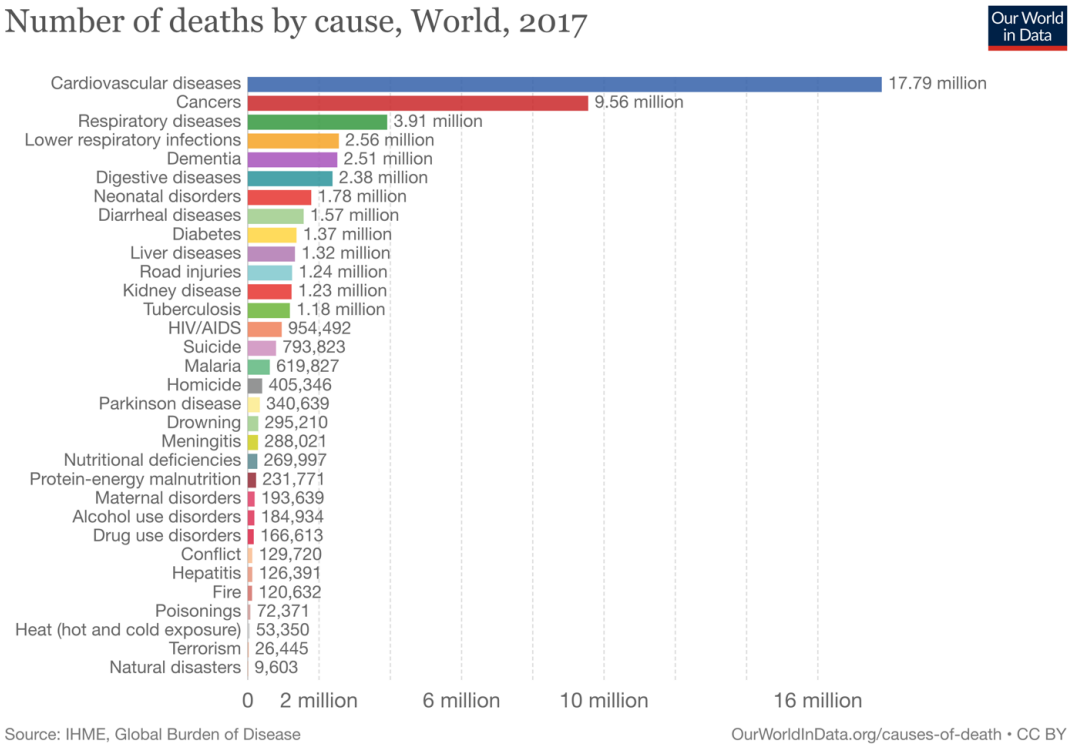

Figure 1.2: Number of Deaths by Cause Worldwide in 2017 [8]

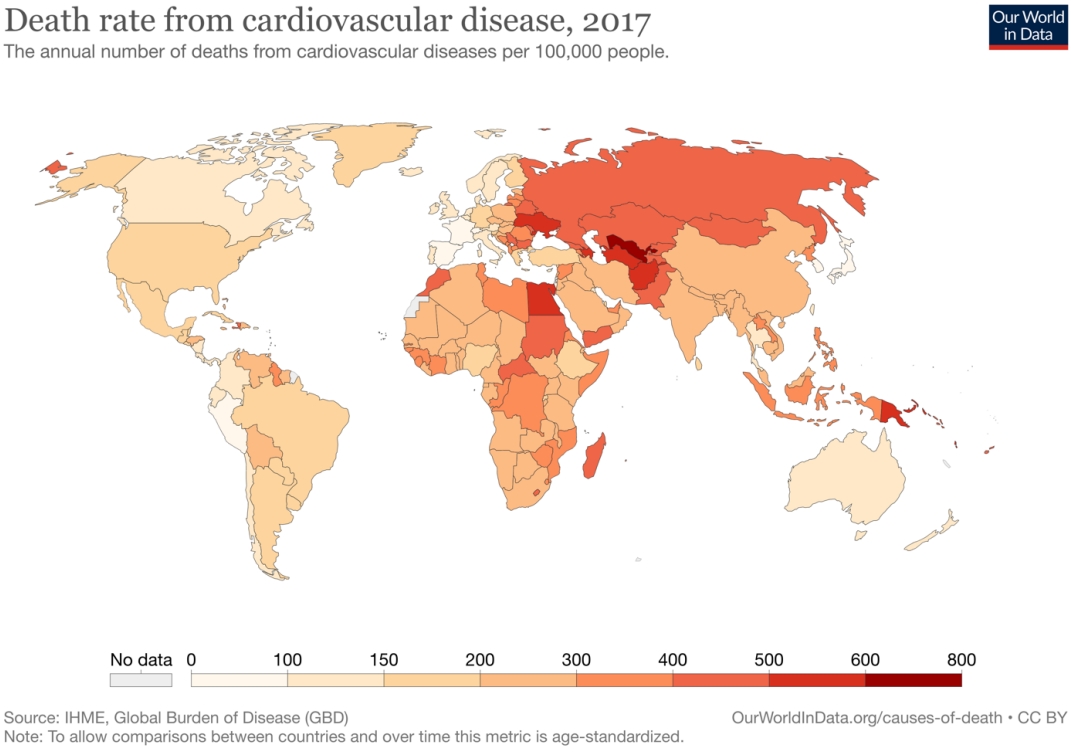

Figure 1.3: CVD Mortality Rate by Country in 2017 [8]

Figure 1.4 shows the distribution of CVD mortalities in males and females in 2017 from the World Heart Federation [9]. Cerebrovascular disease (strokes) and ischemic heart disease (heart attacks) made up over 80% of these deaths, but as mentioned before, this percentage has grown to 85% as of 2020.

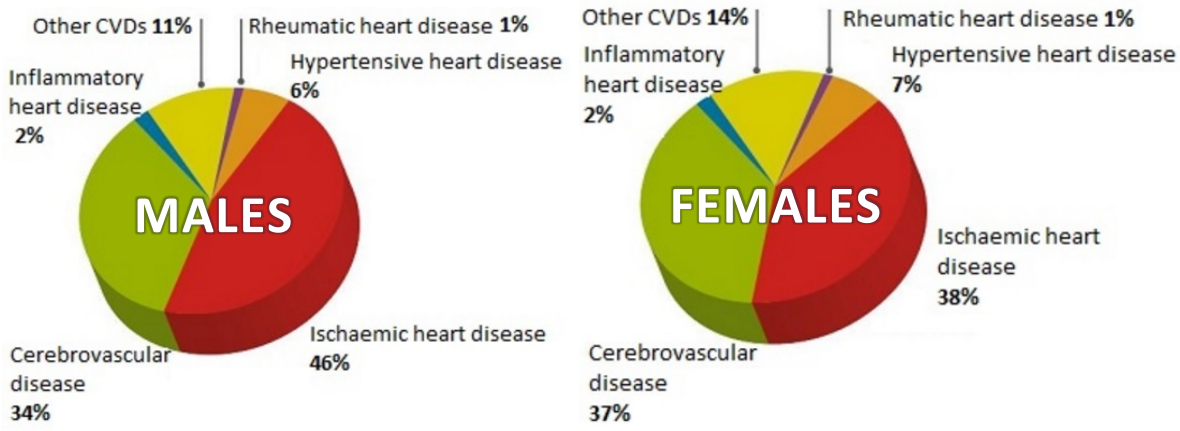

Figure 1.4: Distribution of CVD Mortalities in Males and Females in 2017 [9]

1.4 Risk Factors of CVD

The risk factors of CVD can be categorized as modifiable and unmodifiable. Modifiable factors are those that can be changed based on an individual's lifestyle and habits, while unmodifiable factors are a result of age, gender, and genetics. As people age, the risk of CVD increases naturally. Men have a higher risk for CVD than women, but the risk for women increases after menopause. Additionally, individuals with close family members who have had CVD are genetically predisposed to having a higher risk of CVD [10].

Despite the unmodifiable risk factors, there are many modifiable risk factors that need to be addressed since they are easily preventable with increased public awareness. Table 1.2 describes common modifiable risk factors summarized by the World Health Organization [11].

Figure 1.5 illustrates the causal chain of CVD risk factors also presented by the World Health Organization [12]. These risks can be mitigated with behavioral changes. Studies have shown that increased physical activity results in a 30-50% reduction in CVD risk, a healthy diet results in a 31% reduction, and cessation of cigarette smoking results in a 40% reduction [13].

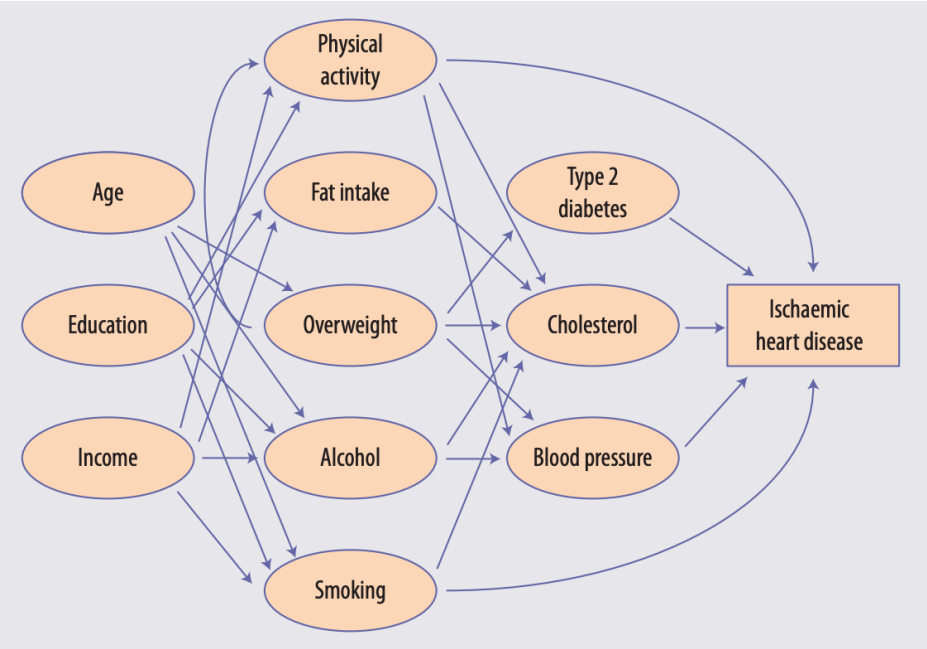

Figure 1.5: Causal Chain of CVD Risk Factors [12]

Risk Factor	Description
Tobacco Usage	There is a direct correlation between CVD risk and amount of tobacco usage. Smoking is estimated to cause nearly 10% of CVDs. Health risks from tobacco use result from both direct consumption of tobacco and exposure to second-hand smoke.
Low Physical Activity	Insufficient physical activity, defined as less than 30 minutes of moderate physical activity at least 5 times a week, or less than 20 minutes of vigorous activity at least 3 times a week, is the fourth leading risk factor for mortality. Regular physical activity is recommended for cardiovascular health.
Excessive Alcohol Consumption	Excessive alcohol consumption is a risk factor for hypertension or high blood pressure, acute myocardial infarction, cardiomyopathy, and other CVDs.
Unhealthy Diet	High dietary intakes of saturated fat, trans-fat, cholesterol, and salt, are linked to high CVD risk. An unhealthy diet often leads to obesity, abnormal blood lipids, or diabetes.
Obesity	Obesity is a growing health problem globally. Studies have shown a strong correlation between obesity and CVD risk factors such as high blood pressure and diabetes.
Hypertension	Hypertension, or high blood pressure, is a major risk factor for heart attacks and strokes. It can also cause heart failure, renal impairment, peripheral vascular disease, and damage to retinal blood vessels.
Diabetes	Diabetes, or raised blood sugar, is a major risk factor of CVD. CVD accounts for about 60% of mortality in people diagnosed with diabetes. Patients with diabetes are two to three times as likely to have a heart attack or stroke.
Abnormal Blood Cholesterol	LDL cholesterol, or “bad” cholesterol, is deposited in walls of arteries and causes atherosclerosis. HDL cholesterol, or “good” cholesterol, removes the bad cholesterol from the walls of arteries. High counts of LDL cholesterol and low counts of HDL cholesterol are directly correlated to increased CVD risk.

Table 1.2: Modifiable Risk Factors of CVD [11]

1.5 Importance of Coronary Arterial Disease and Atherosclerosis

Although there exist many different categories of CVDs, more than 85% of CVD mortalities (heart attacks and strokes) can be attributed to atherosclerosis. Coronary arterial disease (CAD) is the precursor to most heart attacks and strokes, and is caused by narrowing of the coronary arteries that supply oxygen to the heart [14]. Atherosclerosis is a condition in which plaque builds up inside arteries, which hardens and narrows them over time. The plaque deposits are made up of cholesterol, fat, calcium, and other substances in the blood [15]. An illustration of a normal artery compared to a narrowed artery is shown in Figure 1.6 below.

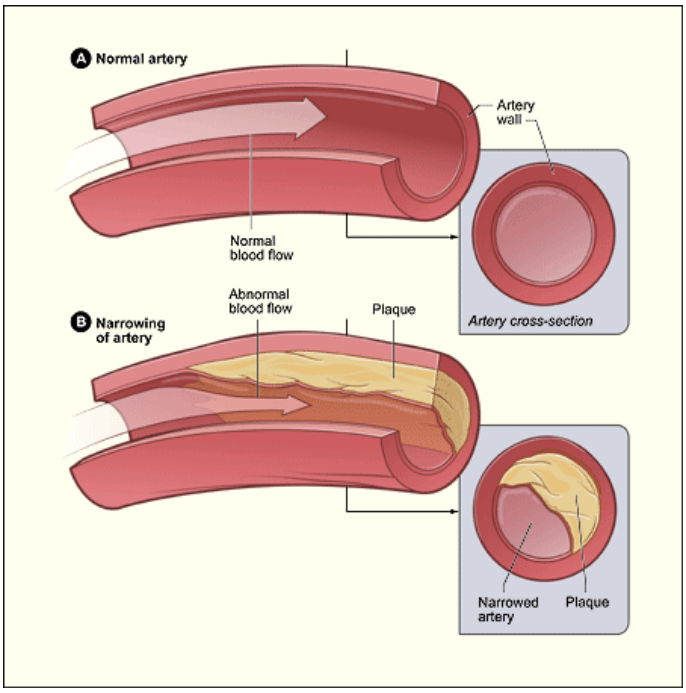

Figure 1.6: Illustration of Plaque Buildup Narrowing and Stiffening Arteries [15]

There are many risk factors that contribute to atherosclerosis, such as age, genetics, high blood pressure, unhealthy diet, smoking, excessive alcohol consumption, lack of physical activity, etc. which were discussed in detail previously in Section 1.4. Some of these factors are unmodifiable, but others are modifiable via lifestyle changes. However, since CAD and

atherosclerosis develop slowly over time, many patients are unaware of it until late stage symptoms occur. Earlier assessment of risk would enable people to become more aware of their health and make an effort to reduce their long term risk. Though there are many aspects of cardiovascular health, our group has decided to focus on addressing atherosclerosis because of its high impact on CVD mortalities.

1.6 Unique Challenges of Detecting Atherosclerosis

Although many CVD risk factors can be mitigated by behavioral change and low-cost medication, it is difficult to detect the disease with existing common solutions without adequate blood test measurements, notably blood pressure and cholesterol levels. Many people around the world do not have access to affordable health care, especially in developing countries. Thus, developing a low-cost non-invasive technology platform for detection of CVD is crucial in diagnosing and treating at-risk individuals.

Unlike many other diseases, a specific challenge of atherosclerosis is that it is often asymptomatic. Because of this, people do not feel any urgency to visit a doctor or seek medical facilities. Thus, it is necessary to develop a scalable platform of screening tools that is accessible and easy-to-use even at home. By screening at home, it is possible to identify individuals that are at risk of atherosclerosis and motivate them to seek treatment.

1.7 Scope of This Thesis

In this thesis, we explore solutions to this problem that have been developed by Dr. Richard R. Fletcher's group, the Mobile Technology Group, at MIT. In particular, I introduce an integrated, scalable platform using non-invasive screening tools that have been developed by previous members of the group.

In Chapters 2-3, I present an overview of existing screening tools developed by other parties, introduce the gap that still needs to be addressed for atherosclerosis specifically, and summarize the individual screening tools that members of our group developed in the past.

In Chapters 4-5, I go into detail about fundamentals of photoplethysmography (PPG), pulse wave analysis (PWA), and pulse wave velocity (PWV). I present a novel method of quantifying PPG waveform characteristics, and discuss improvements to our PWV algorithm.

In Chapters 6-7, I discuss the integration of the screening tools using a server architecture and Android mobile applications to create a scalable platform that can be deployed worldwide.

In Chapters 8-9, I discuss the performance of these metrics in clinical studies. Finally, in Chapter 10, I conclude with a summary of my contributions and future work for this project.

Chapter 2

The Need for Integrated Specialized Screening Tools

2.1 Cardiovascular Measurements

Complete characterization of the cardiovascular system requires evaluating the heart from several different perspectives: mechanical, electrical, and vascular. Traditional gold standard clinical tools include the following:

- Mechanical – Echocardiography
- Electrical – Electrocardiogram
- Vascular – Pulse Wave Velocity tools (Sphygmocor)

It should be noted that all of these tools can be found in a well-equipped large hospital or cardiology center. However, low-cost versions of these tools for the purpose of screening are often lacking.

2.2 Screening vs. Diagnosis

Before discussing the design of cardiovascular assessment tools, it is useful to establish the difference between screening and diagnosis. In general, screening tests are used to identify individuals who may seem healthy, but are actually at risk of having the disease. These tests typically need to be low-cost and easily accessible to large populations. Diagnostic tests, on the other hand, are used to determine whether an identified at-risk patient actually has the disease. The result of a diagnostic test provides a definite diagnosis of the disease [16].

Screening and diagnosis fit into different tiers of a typical public healthcare system in developing countries. In many rural areas, the first point of contact between the members of the community and the primary healthcare system are healthcare workers. Healthcare workers are responsible for screening the community population for potential risks of common diseases, and providing basic medical care related to nutrition, immunization, and family welfare. This is where specialized screening tools are particularly important for assessing CVD risk. Once identified, at-risk individuals are then referred to primary and community health centers that are equipped to perform diagnostic tests and provide treatment [17].

2.2 The Need for CVD Screening Tools

Because the traditional diagnostic tools, such as echocardiograms, CT scans, and blood tests, are generally only available in large health facilities, there is a lack of cardiovascular assessment tools in low-resource areas, as well as in the consumer home setting. CVD screening is important because many CVDs, especially atherosclerosis, are largely asymptomatic. This means that many people who are at risk may not realize it until a severe cardiac event, such as heart attack or stroke, occurs. Widespread, low-cost, and easily accessible CVD screening tools

are necessary for early risk assessment to educate people about their own cardiovascular health conditions, encourage behavioral changes in their daily lifestyle, and enable them to seek out professional medical help if needed. Such screening tools would be useful not only for primary care screening, but also for personal health monitoring in developed countries as well.

To explore this need, in this thesis, we focus specifically on screening tools, not diagnosis. The following sections describe current existing CVD risk screening tools and evaluate their shortcomings. Our goal is to develop integrated tools that address these gaps.

2.3 Existing CVD Risk Score Models

At present, the existing non-invasive methods for CVD screening are generally questionnaires. In this section, we discuss some of the primary non-invasive screening methods used by clinicians and healthcare workers to determine whether an individual is at risk of CVD and needs additional screening with medical equipment.

2.3.1 Framingham Risk Score

One of the gold standard risk score models used today is the Framingham Risk Score. This model was derived from the Framingham Heart Study, a long-term study on cardiovascular health assessment that started in 1948 in Framingham, MA. Though originally planned to last 20 years, the study is still ongoing today due it its impact in understanding the progression of CVD. The first phase of the study involved 5209 participants between the ages of 30 and 62 years old. Every two years, study participants took medical tests and answered detailed lifestyle questions. Researchers monitored which participants developed heart disease and which did not. In 1971, a second cohort of 5124 individuals, consisting of the offspring of the original group and their

spouses, was added to the study and monitored in a similar way. Most recently in 2002, a third generation cohort of size 4095, children of the second cohort, was added to the study. The study findings greatly influenced the scientific understanding of CVD risk factors [18].

In 1998, Wilson et al. developed a scoring method for assessment of CVD risk based on this study, known as the Framingham Risk Score. The model takes input factors of age, gender, blood pressure, blood cholesterol, smoking habits, diabetes diagnosis, and outputs an overall score indicating an individual's 10 year risk of developing CVD [19]. This risk score model remains one of the most popular and most often validated models.

2.3.2 WHO Risk Prediction Charts

Similar to the Framingham Risk Score model, the World Health Organization (WHO) has also developed a set of multi-factor screening charts that can identify individuals at risk of CVD based on age, gender, smoking habits, blood cholesterol, and diabetes diagnosis. Example screening charts are shown in Figure 2.1. Unlike the Framingham Risk Score, however, WHO has different charts available for all of its subregions to account for ethnic and regional differences [20].

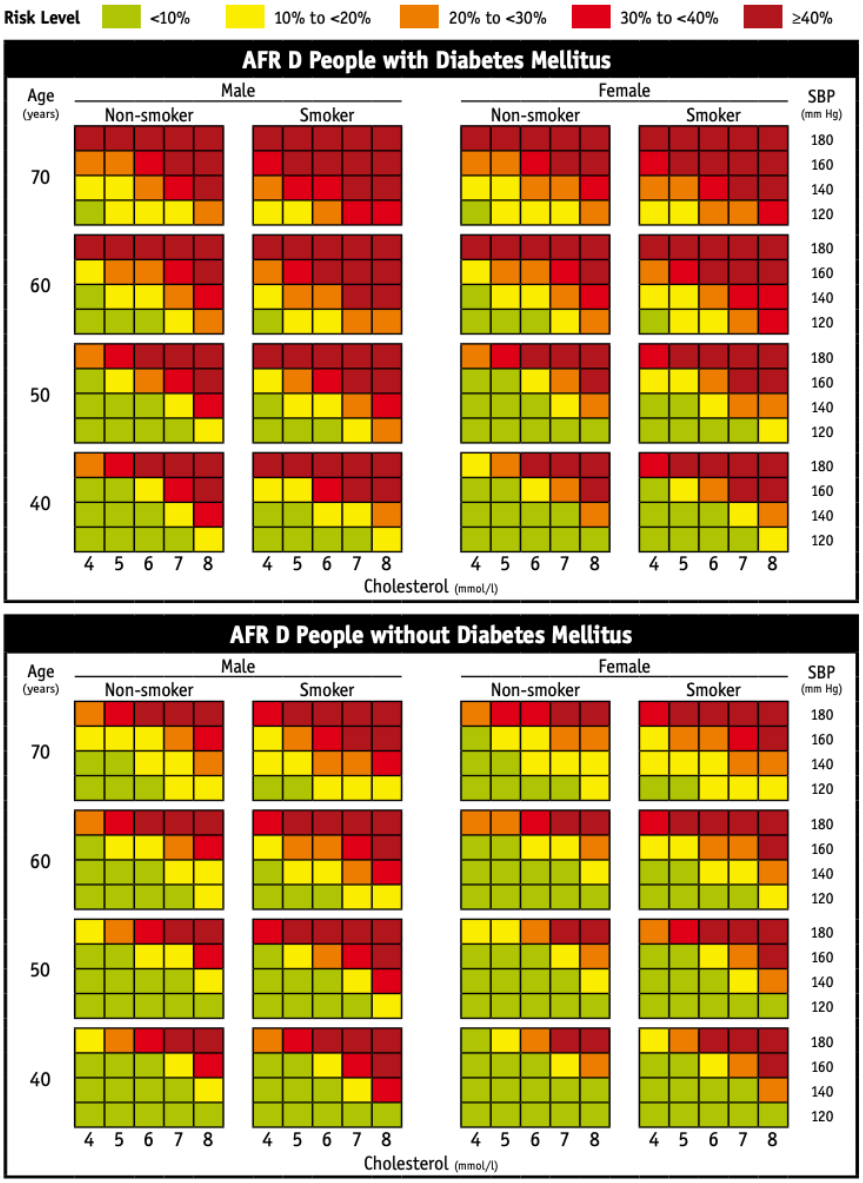

Figure 2.1: Example WHO Risk Prediction Charts

2.3.3 Other Risk Score Models

Other risk score models have been developed to address the lack of ethnic diversity in the Framingham Risk Score. As mentioned previously, one of these is the WHO Risk Prediction Charts. Additionally, the QRISK2 Score is a similar calculation as the Framingham Risk Score, but is calibrated to the United Kingdom population, and includes additional factors such as past

heart and kidney health history, BMI, and arthritis status [21]. Another model, the Reynolds Risk Score, was designed to improve fit for women over the age of 45. It also showed improvement in prediction accuracy for women of African American descent [22].

2.4 Shortcomings of Existing CVD Risk Score Models

Many of the existing models, especially the Framingham Risk Score, were not developed to account for differences in genetics, ethnicity, regional, and socioeconomic factors. The Framingham Study participants were primarily white males of European descent. The QRISK2 score tailors to the UK population specifically. In addition, a major drawback existing of the risk score models is their dependency on blood pressure and blood cholesterol. Obtaining blood cholesterol levels requires an invasive blood test and medical laboratory equipment, which are not widely available to everyone. Blood pressure, a seemingly trivial measurement, actually requires proper clinical training to get an accurate reading. A variety of factors can cause inaccuracies in blood pressure measurement. These include patient posture, size of the cuff, location of cuff placement, and accuracy of the measuring device itself [23]. Hence, these two measurements have made the risk score models much less accessible than intended, and hindered many people from understanding their CVD risk.

2.5 Existing Mobile Technology Solutions

2.5.1 Current Mobile Apps for Cardiovascular Health

As the use of smartphones has become extremely widespread, many mobile applications have been developed for monitoring cardiovascular health. These applications are either self-

contained or involve using an external recording device in combination with the app. Currently, the two main concepts used in monitoring heart rate, heart rate variability, and atrial fibrillation with mobile technology are smartphone-based PPG and external handheld ECG recorders [24].

PPG is a non-invasive method of measuring an individual's pulse using a light source and a photodetector. It uses optical techniques to detect changes in blood volume, which corresponds to the pulse waveform. Since nearly all current smartphones are equipped with high-resolution cameras, processors, and LED flashlights, a smartphone-based PPG is easily accessible. For this method, a subject covers the smartphone camera lens and flashlight with a fingertip, and the phone camera records a continuous video of light reflected from the finger. The changes in red, green, and blue color values during each frame results in a PPG signal [25]. Table 2.1 lists some of the current state-of-the-art mobile apps.

Application	Description	Measured Signals
KardiaMobile [24]	Mobile app and finger pad sensors attached to phone used for monitoring atrial fibrillation	ECG
CardiioRhythm [24]	Analyzes finger and facial PPG signals for detection of atrial fibrillation	PPG
FibriCheck [24]	Uses finger PPG and a single-lead ECG to detect atrial fibrillation	ECG, PPG
Instant Heart Rate [26]	Popular Android app that measures heart rate	PPG
Runtastic Heart Rate [26]	iOS app similar to Instant Heart Rate	PPG

Table 2.1: Mobile Applications for Cardiovascular Health Monitoring

2.5.2 Wearable Sensors for Health Monitoring

In addition to mobile apps, in more developed countries, wearable technology has also emerged as a popular tool for monitoring our health. Recently, wearable biosensor systems for cardiovascular health monitoring have been introduced for personal health management and continuous monitoring by clinicians for diagnosis and treatment. These systems are low-cost, and comprised of various types of small non-invasive physiological sensors and transmission modules. Table 2.2 lists some of the recently developed wearables that measure signals correlated to cardiovascular health. The majority of these devices measure ECG, or electrocardiogram, which shows the electrical activity of the heart.

2.6 Shortcomings of Existing Mobile Technology Solutions

The majority of screening tools reviewed previously focus on measuring ECG and heart rate, and many of them are designed to detect atrial fibrillation. Although there are also some apps that claim to measure blood pressure with just a smartphone, studies have shown that these apps can be highly inaccurate, with up to 77.5% false negative classification rate of hypertensive individuals [30]. While helpful, these metrics do not directly screen for atherosclerosis, which is the precursor to heart attacks and strokes, accounting for 85% of all CVD mortalities. Thus, despite the numerous mobile applications widely available, there exists an immediate need to address the lack of targeted screening of atherosclerosis.

Device	Description	Measured Signals
AMON	Monitoring device using GSM link worn on the wrist for high-risk cardiac-respiratory patients	ECG, heart rate, blood pressure, activity
MyHeart	Textile with conductive yarns and electronic sensors on clothes and a belt used for preventative early diagnosis of CVD	ECG, respiration, activity, other vital signals
HeartToGo	Device for individualized remote CVD detection using Bluetooth and GPS	ECG, activity
Personal Health Monitor	A heart-attack self-test for CVD patients that uses Bluetooth and GPS	ECG, blood pressure, activity
Wearable ECG for Arrythmia Monitoring	Project in Norway for continuous monitoring and remote detection of cardiac arrythmias in CVD patients	ECG
Ring Sensor [27]	A PPG ring sensor for monitoring cardiovascular health	Heart rate, heart rate variability, oxygen saturation
Kardia [28]	ECG monitoring device that connects to a nearby smartphone for remote interpretation of ECG data	ECG
Cardionet MCOT [28]	A wearable device that measures ECG via cellular connection and detects cardiac arrhythmias	ECG

Table 2.2: Wearable Sensors for Cardiovascular Health Monitoring [29]

2.7 Summary

In this chapter, I discussed the difference between screening and diagnosis, and established the importance of having more accessible CVD screening tools. I evaluated existing risk score models and mobile technology solutions, and addressed their shortcomings. In the following chapter, I will discuss our group's proposed solution for a specialized integrated CVD toolkit. I will give an overview of prior work done in our group, and introduce my contributions to the project.

Chapter 3

Proposed Solutions for CVD Screening

We propose a holistic cardiovascular screening mobile platform that is low-cost, scalable, and addresses the shortcomings of existing screening tools discussed in Chapter 2. I start by discussing prior work done by our lab on CVD screening tools, and then introduce new developments to the work. Although the tools were initially designed for use in low-resource and rural places in India, it is important to note that the integrated platform is useful for CVD risk assessment even in developed settings.

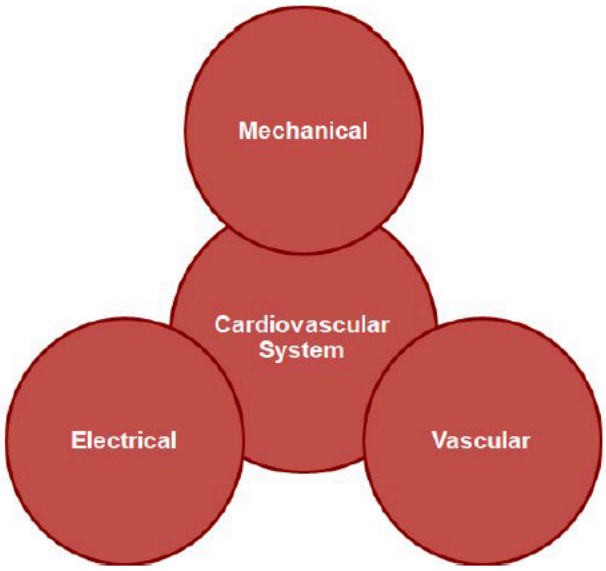

Figure 3.1: Three Interconnected Perspectives of the Cardiovascular System

3.1 Prior Work from the Mobile Technology Group

As discussed in Section 2.1, a complete evaluation of the cardiovascular system include different categories of measurements: electrical, mechanical, and vascular, shown in Figure 3.1. Our group has a developed a variety of low-cost tools to serve this purpose. These tools include a questionnaire, various hardware tools, pulse wave analysis and pulse wave velocity algorithms, a machine learning algorithm, and a server framework, which are summarized in the following sections. To validate the algorithms, previous M.Eng. student, Niccolò Pignatelli started an ongoing clinical study at the Sengupta Hospital and Research Institute in Nagpur, India. I will discuss the study design and most recent results of this clinical study in Chapter 8.

3.1.1 CVD Risk Screening Questionnaire

We developed an Android mobile screening application based on the Framingham Risk Score model. Clinicians or patients fill out an individual questionnaire on the mobile phone that takes in information such as age, gender, blood pressure, blood cholesterol, diabetes diagnosis, and smoking frequency, and gives a prediction of a person's ten year risk of developing CVD. However, since this model is a general screening guide, it does not accurately measure the extent of CVD progression, and cannot screen for atherosclerosis specifically. The method also requires an invasive blood test to determine the blood cholesterol level, which is not widely available to everyone. For these reasons, we kept the Framingham Risk Score as a low-level reference calculation, and supplemented it with additional devices and algorithms for a more accessible, detailed, non-invasive screening for CVD.

3.1.2 Mobile Stethoscope

For mechanical evaluation of the heart, Pignatelli developed a mobile stethoscope using the principles of phonocardiography to screen for abnormal heart sounds, which may be due to congenital problems or valvular issues. He also trained a machine learning model to recognize abnormal heart sounds in the recordings [31]. Figure 3.2 shows a prototype of the mobile stethoscope.

Figure 3.2: Mobile Stethoscope

3.1.3 Microwave Doppler Sensor

For a better evaluation of cardiac function, Pignatelli also developed a microwave doppler device, which is a low-cost alternative to the heart echocardiogram. Using this tool, we can record the impedance and reflected power from a probe placed on the chest, and which monitors movements of the heart muscle [31].

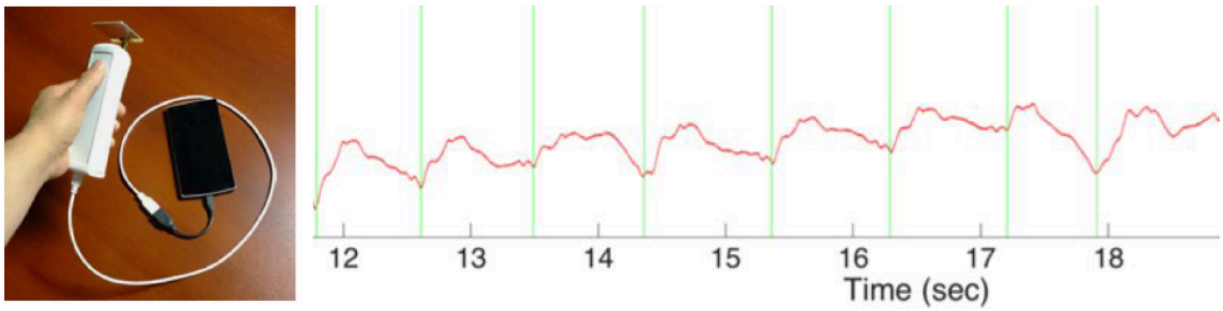

Figure 3.3: Microwave Doppler Sensor (left) and a Sample Collected Signal (right)

3.1.4 Smartphone-based PPG

In recent years, our group has developed a variety of mobile software tools to record a PPG waveform using the mobile phone camera. This technique enables highly scalable data collection without the need for any external equipment. Previous students, such as Josef Biberstein, have developed a mobile phone applications for several different clinical studies. Figure 3.4 shows the mobile application in use and a sample collected signal.

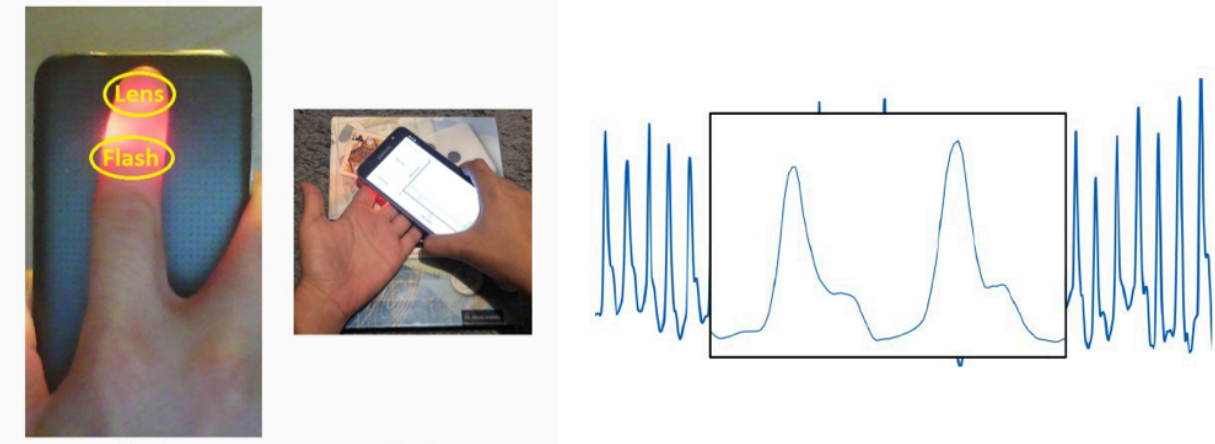

Figure 3.4: PPG Camera Mobile Application Demonstration (left and middle) and Sample Collected Finger PPG Signal (right)

3.1.5 PPG Pulse Wave Analysis

Pulse wave analysis (PWA) has traditionally been performed using tonometry of the radial artery in a human forearm. This technique uses an external pencil-like probe to measure pressure waves and generate an average central aortic pulse waveform [32]. Instead of using tonometry, our group has performs PWA using the PPG waveform instead of the traditional arterial pressure waveform. For example, previous M.Eng. student, Botong Ma, developed the initial code and algorithms to process the raw data collected by the mobile phone and extract PWA features correlated to the extent of atherosclerosis [5].

3.1.5 Multi-site PPG and Pulse Wave Velocity

In addition to PWA, our group has also explored lower-cost methods of measuring PWV. Instead of using an inflatable cuff, a tonometry pressure sensor, our group has explored the use of low-cost PPG probes that can be clipped onto different parts of the body. For this purpose, our group has designed an external PPG device named the NAJA, which consists of three PPG probes and a central interface board. By clipping the probes to an individual's ear, finger, and toe, and plugging the main board into a smartphone, we can measure the person's PWV. Unlike other PWV measurement systems that use the ECG signal as a timing reference, our measurement system makes use of the ear PPG signal. Figure 3.5 shows a NAJA probe and proper probe placements on a patient.

Previous M.Eng. student, Botong Ma also developed algorithms to calculate PWV in Python from the collected signals. She then developed a machine learning algorithm to classify healthy versus non-healthy patients based on PWV [5].

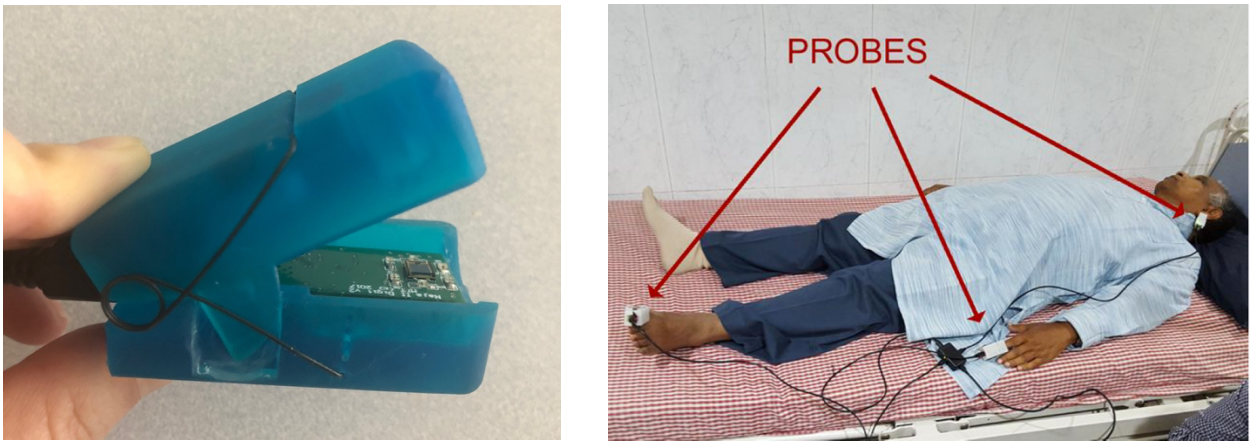

Figure 3.5: A NAJA Probe (left) and Demonstration of Probe Placements (right)

3.1.6 Server Framework

Another previous M.Eng. student, John Mofor, created a server framework, PyMedServer, that allows for large scale collection of medical data, and can be customized for the needs of individual projects [33]. We present a high level architecture overview of the integrated platform using PyMedServer in Section 3.3. Chapter 7 discusses the customizations for the CVD server in detail.

3.2 Limitations of Previous Work

Although particular sections of our cardiovascular screening tools have been previously demonstrated, a considerable amount of work still remained to integrate all these components into a single practical data collection system.

Most of the tools mentioned above only used the mobile phone as a measuring and recording device, but data saved to the phone still needed to be manually extracted onto a computer for pre-processing and analysis. Since many of our algorithms, such as PWA and PWV, are calculation intensive, not all mobile phones have enough processing power to run them. This extra manual step made it difficult to keep track of data and results once the number of data points increased. Thus, it is necessary to integrate these individual measurement components with a custom server based on Mofor's PyMedServer framework. The mobile phones are able to record and upload data to the server. The server then runs the algorithms on selected data sets, and returns analyses results for display on the mobile phone. With this integration, we are able to create a scalable and practical solution that can be deployed worldwide.

3.3 Contributions of This Thesis

For this thesis, I have chosen to focus on integrating a few selected non-invasive measurements including the questionnaire, the camera finger PPG for PWA, and the NAJA device for PWV to create a scalable platform that can be deployed globally.

First, I have refined the PWA and PWV algorithms to be able handle a wider variety of pulse waveforms and return a more accurate calculation. In particular, I developed a novel method of scoring PWA waveforms as they progress from healthy to unhealthy. PWA and PWV are discussed in detail in Chapters 4 and 5 respectively.

Additionally, each of the standalone Android applications has been updated to be compatible with the most recent version of Android and also to be able to communicate with the server. Using PyMedServer-Android libraries, I have created a CVD screener mobile application bundle, which includes a container application that handles user authentication, launches each standalone measurement application, and runs server analyses. Further details on the mobile application features are discussed in Chapter 6.

The current CVD server platform has been constructed based on the PyMedServer architecture and customized to support these measurements. Instead of requiring manual download of the data from the mobile phone to a laptop for data processing, I have automated this process to enable analysis using a remote server. Figure 3.6 shows a high level overview of the CVD screening platform architecture. Details regarding the API structures and server features are presented in Chapter 7.

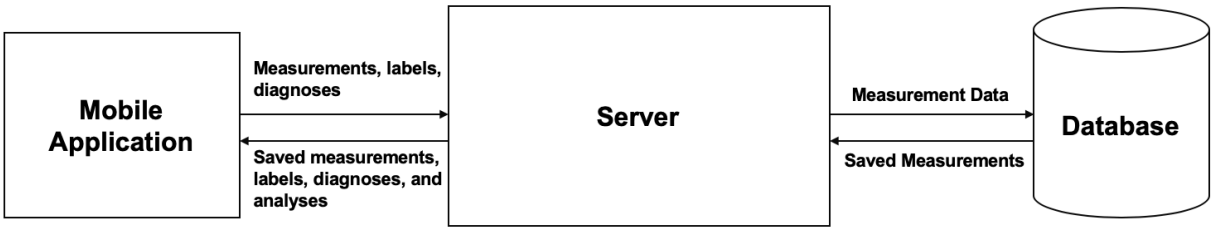

Figure 3.6: CVD Screening Platform Architecture

Finally, I have conducted a separate clinical studies to validate the new PWA algorithm and demonstrate the differences between four different classifications of cardiovascular health. I also collected and analyzed additional data for PWV as part of the ongoing clinical study at the Sengupta Hospital and Research Institute. I present the IRB-approved study protocols and analysis results in Chapters 8 and 9.

3.4 Summary

In this chapter, I summarized prior work done on CVD screening tools in our group. I then presented the limitations of this previous work, and highlighted my contributions in this thesis which address these limitations. In the next chapter, I will discuss PWA in detail, including its applications to CVD screening, and the novel scoring metric I developed.

Chapter 4

Pulse Wave Analysis (PWA)

4.1 Fundamentals of PPG

To understand PWA, we first introduce photoplethysmography (PPG), which is a non-invasive method of measuring changes in blood volume in the human body. The basic PPG measurement configuration consists of a light source and photodetector, and relies on optical detection of changes in blood volume during a cardiac cycle in the microvascular bed of biological tissue. Light shines through the tissue, and a photodetector detects the amount of light that is either reflected or absorbed by the blood and tissues. As blood flows through the blood vessels, the minute changes in blood volume can be observed as a change in the amount of light received by the photodetector. These changes result in a PPG signal, in which blood flow during the systolic and diastolic phases make up the pulsatile AC component and the structure of the blood vessels and average blood volume make up the steady DC component [34]. Figure 4.1 plots the components of a PPG signal.

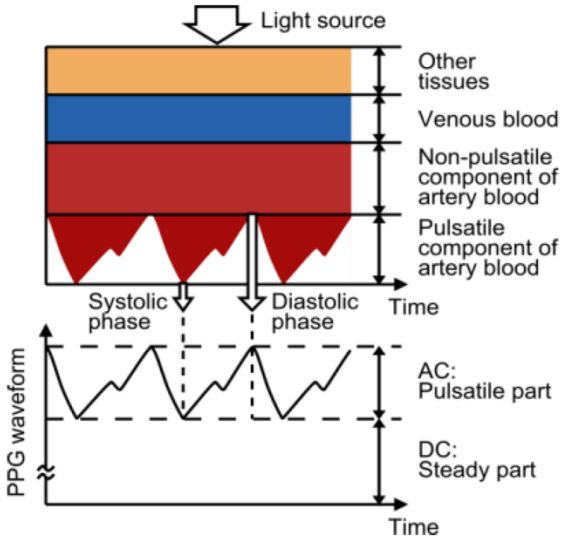

Figure 4.1: Variation in Light Attenuation and the Resulting PPG Signal [1]

There are two methods of configuring the light source and photodetector:

- Reflectance: the photodetector detects light reflected from the tissue and bones
- Transmission: the photodetector detects light that is transmitted through the tissue and bones

Figure 4.2 shows example configurations for finger PPG. Since the transmission method relies on light being able to pass through the tissue, transmission PPG sites are generally limited to fingertips, earlobes, and toes. Using the reflectance method, on the other hand, gives more freedom in placement [35].

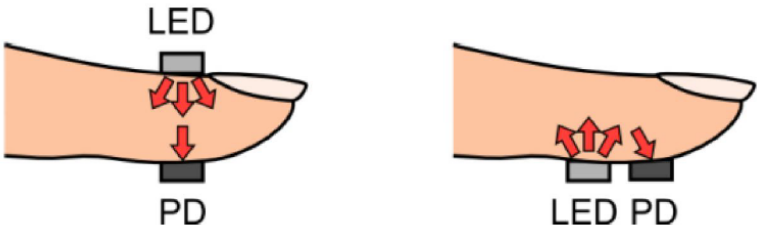

Figure 4.2: Transmission PPG Method (left) vs Reflectance PPG Method (right) [5]

4.2 Features of the PPG Waveform

A typical PPG waveform consists of two phases which are the rising edge due to a systolic contractions, and the falling edge as a result of the diastolic relaxation of the heart [36]. Figure 4.1 shows an example PPG waveform and its fundamental features.

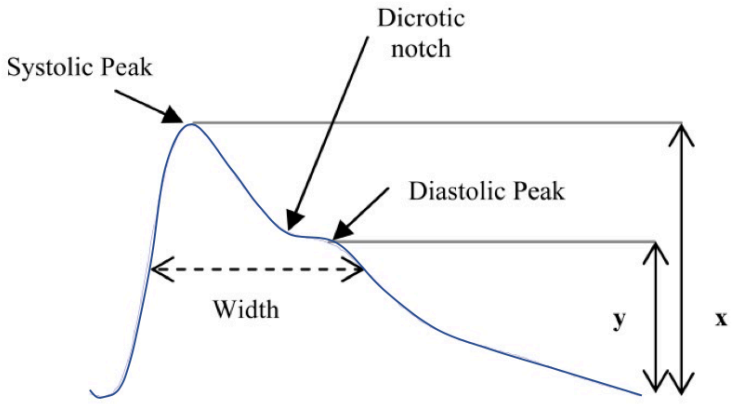

Figure 4.3: A Typical PPG Waveform and Features [36]

In young and healthy individuals a second small peak often appears after the main systolic peak, during the diastolic phase. This undulation occurs because the PPG waveform is actually a superposition of the outgoing systolic wave along the central artery and the reflection of the pulse wave from the arterial tree at the base of the central artery. In young healthy individuals, the reflected wave will reach the heart just as it is relaxing in its diastolic phase [5]. What appears as the "diastolic peak" is thus the reflection of the original systolic contraction of the heart.

The valley or undulation between the systolic peak and the diastolic reflection is often informally referred to as the "dicrotic notch." However, this is misnomer. The true dicrotic notch is the sharp dip in the arterial pressure that occurs when the aortic valve opens. Nevertheless, it has become a convenient term to refer to the transition region between the systolic and diastolic phases.

4.3 PPG Waveforms in Relation to Atherosclerosis

4.3.1 Classifications of PPG Waveforms

As mentioned in Chapter 1, atherosclerosis is a category of CVD characterized by stiffening of the arteries, and is the precursor to strokes and heart attacks. For the purpose of this chapter, it is interesting to note how the shape of the PPG waveform changes with increasing age and arterial stiffness. Intuitively, we may expect that the increased arterial stiffness results in increased pulse wave velocity, causing the reflected pulse wave in the diastolic phase to return to the heart prematurely. As a result, we expect decreased separation between the systolic and diastolic phases of the pulse, such that the "dicrotic notch" is eventually no longer visible.

Indeed, the evolution of the PPG pulse wave as a function of disease progression was first described by Dawber et al. The four canonical stages of the waveform described by Dawber are shown in Figure 6.4. A young healthy individual's pulse waveform starts as Class I and gradually evolves toward Class IV with increasing age and arterial stiffness [37].

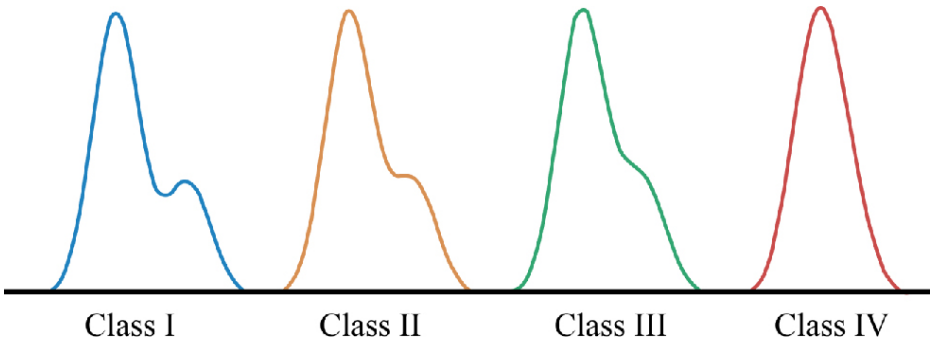

Figure 4.4: Four Classifications of PPG Waveforms First Proposed by Dawber et al. [38]

As a pulse waveform evolves from Class I to Class IV, the leading rising edge becomes more rounded and the dicrotic notch feature deteriorates. The work in our group has focused on two

main features of the PPG waveform that can be used to quantify the progression and degree of atherosclerosis and arterial stiffness. These features are described below.

4.3.2 Rising Edge of PPG Waveform

One PWA feature we have chosen to analyze is the steepness of the rising wave, or what we call the rising slope. The rising slope is correlated to crest time of the wave, which is defined as the time starting from the foot of the waveform to its peak [39]. We can expect this slope to decrease with increased arterial stiffness because the reflected diastolic pulse is superimposed on the systolic pulse, causing the rising edge to become more rounded. Figure 4.3 illustrates this effect by comparing arterial pressure waveforms from a young person and an elderly person. We can see that in the advanced stages of atherosclerosis, the reflected pulse wave travels so quickly that it arrives at the heart during the end of the systolic phase. In addition to causing additional stress on the heart, this reflected wave also causes the systolic peak to be wider and have a more rounded leading edge. We expect the PPG waveform to exhibit similar changes.

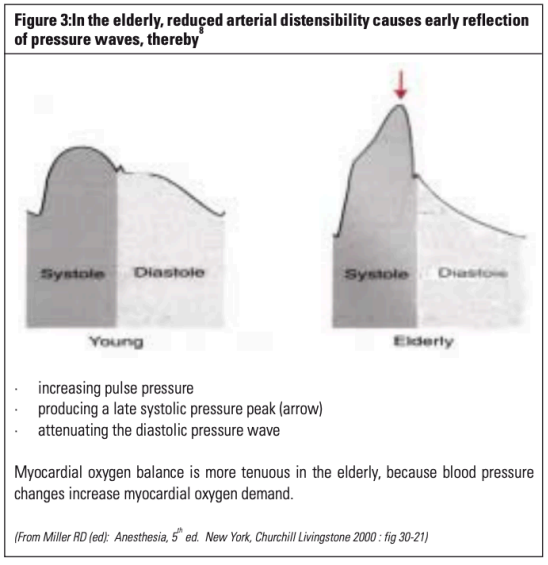

Figure 4.5: Sample Arterial Pressure Waveforms, showing increasing Rising Slope with Age and Arterial Stiffness [40]

4.3.3 Falling Edge of PPG Waveform

In the early stages of atherosclerosis, perhaps the most significant change in the PPG waveform occurs in the trailing or falling edge of the PPG pulse. The falling edge is not monotonic and may include an undulation where the systolic wave meets the reflected wave. As the central artery become stiffer, and the reflected wave travels faster, we see from the Dawber canonical peak stages that the falling edge undergoes a significant transformation.

4.4 Quantification of PWA Features

In order to explore various methods to quantify changes in the PPG pulse shape, I selected sample PPG data from prior work in our group based on the Dawber canonical peaks. I then calculated the first and second derivative of these peak waveforms to see how the derivatives and zero crossings change as a function of disease progression. This is shown in Figures 4.5 and 4.8.

4.4.1 Calculating Changes in the Rising Edge

In order to calculate changes in the rising edge, we have a few options. The initial work in our group to quantify the rising edge used a linear approximation from the foot of the curve to the systolic peak of the curve. By calculating the slope of this linear approximation, it was possible to derive a score for the shape of the rising edge [5]. While this method works for general pulses, it was not robust against the variability in the lower tail of the waveform.

For this thesis, I made an improvement of this calculation by using the second derivative of the PPG waveform. This has the advantage of being more robust against high variability in the

lower tail of the curve. The current algorithm for quantifying the rising edge of the PPG pulse can be described mathematically as follows referencing Figure 4.4:

$$Rising\ Edge\ Area\ Ratio = \left| \frac{\int_{t1}^{t2} f''(x)}{\int_{t1}^{t2} f(x)} \right|$$

Visually, the algorithm computes the area ratio between the shaded purple region and shaded blue region in Figure 4.6. We chose these boundaries of integration because the area of the second derivative represents the maximum slope of the rising edge. To normalize this area and create a usable score, we chose to integrate the original PPG signal from the peak of the first derivative to the peak of the original curve, marked as t_1 and t_2 in Figure 4.6 since these two points are consistently present in all PPG curves.

Figure 4.7 shows the progression of the rising edge area ratio parameters with deteriorating cardiovascular health. As a PPG curve progresses from Class 1 to Class 4, we can expect the area of the second derivative to decrease since the rising slope decreases, and the area of the original curve to increase because the pulse waveform becomes wider. Thus, the overall rising edge area ratio decreases with increased atherosclerosis.

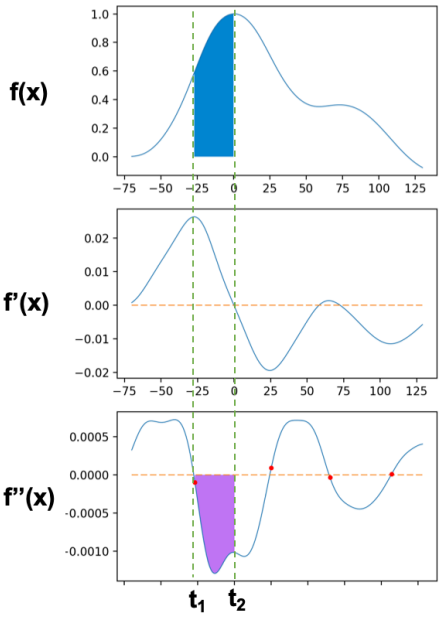

Figure 4.6: Areas used in Rising Edge Area Ratio Calculation

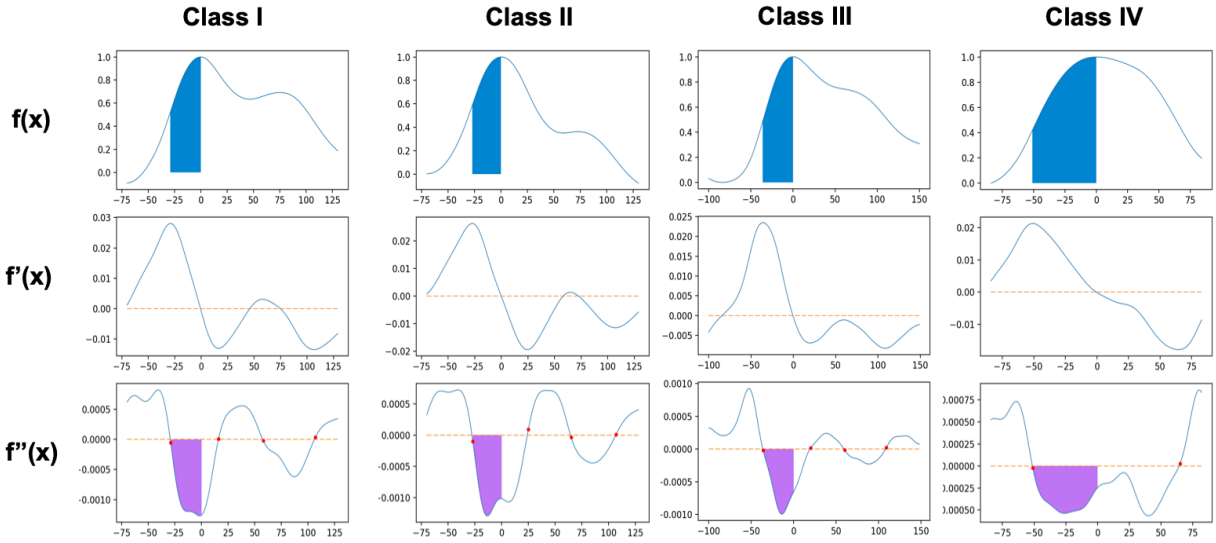

Figure 4.7: Rising Edge Area Ratio Parameters for Four Classifications of PPG Waveforms

Using this area ratio, we calculate a total Rising Edge Parameter value as follows:

$$Rising\ Edge\ Parameter = Rising\ Slope + Rising\ Edge\ Area\ Ratio$$

We chose to include the rising slope in the calculation because in our clinical study discussed later in Chapter 8, we found that although we could see a trend between the different clinical health classifications, the Rising Edge Area Ratio itself, adding the Rising Slope reduced the variance in scores per category. Since area and slope are fundamentally different units, we scaled the Rising Slope to be on the same order as the Rising Edge Area Ratio before summing them.

4.4.2 Falling Edge Parameters

The falling edge of the PPG waveform represents a large challenge of quantification, since this part of the PPG curve exhibits a variety of changes as a function of disease progression. Changes in the falling edge of the curve can be expressed in terms of several parameters that capture the changes occurring in the diastolic phase of the PPG pulse waveform.

The original implementation of our PWA scoring algorithm employed a method that characterized the dicrotic notch by calculating the time delay between the systolic peak and the diastolic peak using zero crossings of the first derivative [5]. We named this parameter the S-D Delay. Figure 4.8 illustrates the correlation between the systolic and diastolic peaks and the first derivative zero crossings.

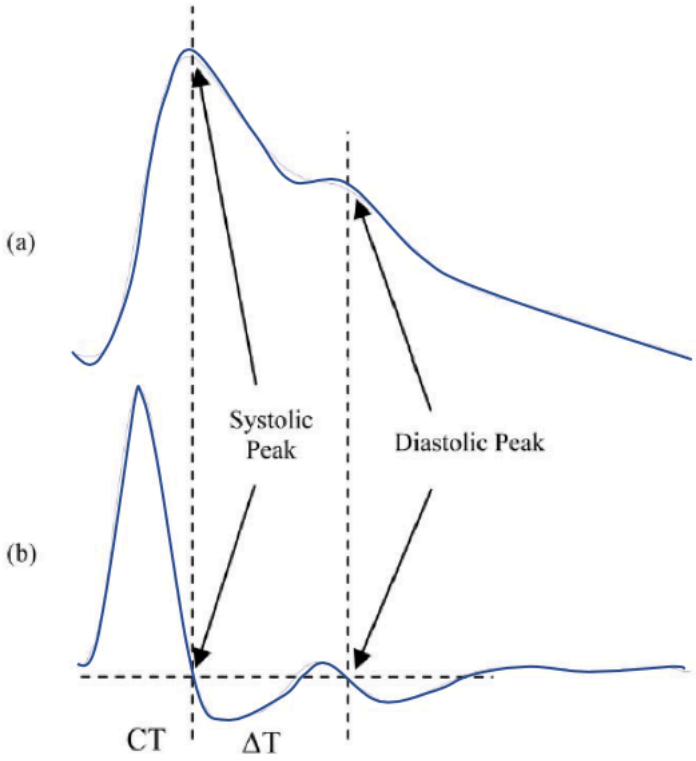

Figure 4.8: (a) Systolic and Diastolic Peak of PPG Waveform, and (b) First Derivative of PPG Waveform and Zero Crossings [36]

While this method worked reasonably well for individual peaks, which exhibited a distinct dicrotic notch, we discovered that this method was not very useful for PPG waveforms that lacked any undulation in the falling edge of the PPG curve. As a result, it was necessary to explore a new algorithm.

My scoring metric, called the S-D Parameter, uses areas from the second derivative and the original PPG curve to calculate an area ratio capable of quantifying the falling edge of any PPG curve. This S-D Parameter can thus be calculated mathematically as follows referencing Figure 4.7:

$$SD\ Parameter = \frac{|\int_{t3}^{t4} f''(x)| + |\int_{t4}^{t5} f''(x)|}{\int_{t1}^{t2} f(x)}$$

Visually, the algorithm computes the area ratio between the magnitude of shaded orange region and shaded blue region in Figure 4.9. The orange region with positive area quantifies the concave-up region in the falling edge of the PPG curve. Similarly, the orange region with negative area quantifies the concave-down region of the falling edge. It is important to note that we take the magnitude of this negative area and sum it with the positive area because the score should reward both qualities.

Just like the Rising Edge Area Ratio, to normalize this area and create a usable score, we chose to integrate the original PPG signal from the peak of the first derivative to the peak of the original curve, marked as t_1 and t_2 in Figure 4.9 since these two points are consistently present in all PPG curves.

Figure 4.10 shows the progression of S-D Parameter with deteriorating cardiovascular health. As a PPG curve progresses from Class 1 to Class 4, we can expect the magnitude of the areas of the second derivative to decrease since the undulation becomes less pronounced. Eventually, this area will become zero when there is no undulation. At the same time, we expect the area of the original curve to increase because the pulse waveform becomes wider. Thus, the overall S-D Parameter decreases with increased atherosclerosis.

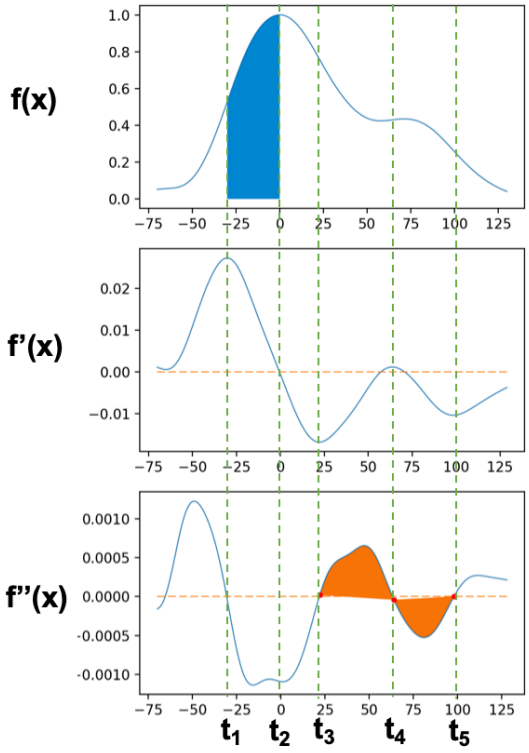

Figure 4.9: Areas used in S-D Parameter Calculation

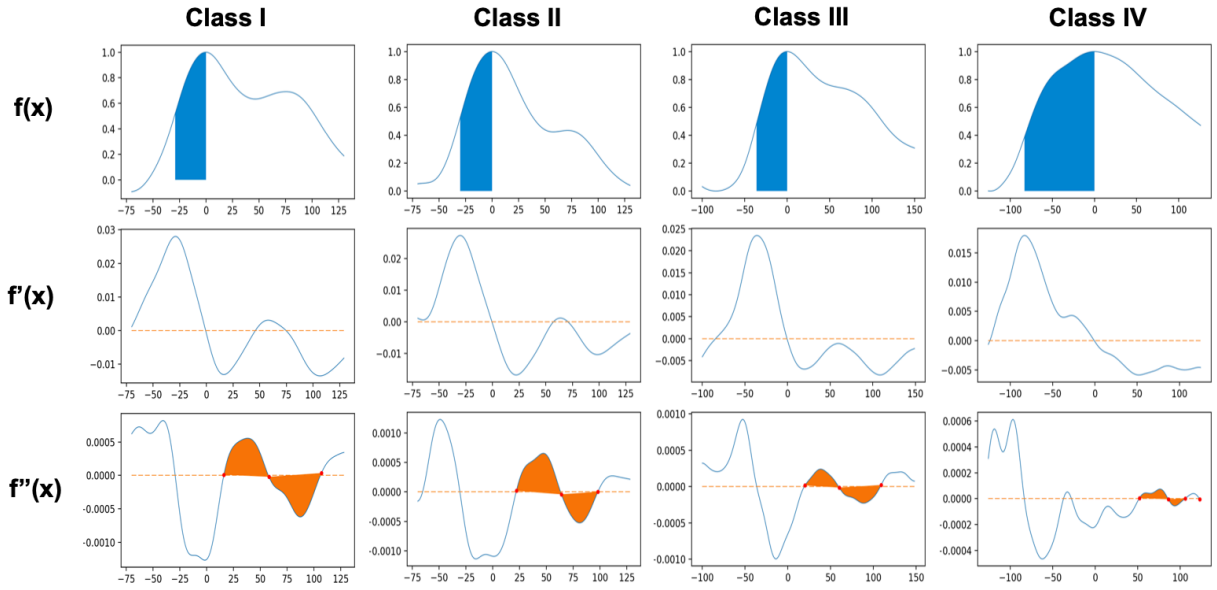

Figure 4.10: Areas used to Calculate S-D Parameters for Four Classifications of PPG Waveforms

4.4.3 Creating a Composite PPG Score

In order to fully characterize a PPG waveform from a patient, it is then useful to combine the rising and falling edge parameters to derive a composite score for the patient. As discussed previously, we speculate that the S-D parameter appears to be most useful in detecting the early stages of atherosclerosis, and the Rising Edge Parameter is more useful in detecting the later stages of atherosclerosis.

If we wish to create a binary classifier to detect a specific severity of atherosclerosis, it would be possible to simply use the rising edge and S-D parameters as features and create a machine learning model. However, if we wish to derive a continuous figure of merit parameter, such as a "PWA Score", then we need to combine these parameters in a logical expression.

For the purpose of simplicity, we can define the PWA Score as follows:

$$PWA\ Score = Rising\ Edge\ Parameter + SD\ Parameter$$

Of course, it is possible to create a linear combination of these parameters with adjustable coefficients if required for clinical use.

This resulting PWA Score represents a convenient way to characterize an arbitrary PPG waveform and provide a quantitative indicator of vascular health. It is also important to note that the PPG waveform analysis presented in this chapter can be applied to both a conventional fingertip probe as well as finger PPG data collected from a smartphone camera.

4.5 Software Implementation

4.5.1 Software Tools

All the algorithms presented here were implemented in Python3 with the Numpy library, and the resulting software was installed on a cloud server. In Chapters 6 and 7, I describe how the mobile phone application for PPG measurement is integrated with the Python algorithm on the server.

4.5.2 Deriving a Canonical PPG Peak from a Patient

For data collection, a practical challenge in quantifying PPG waveforms is that the PPG measurement can be somewhat fragile and has some degree of variability, based on the measurement procedure as well as motion artifacts caused by the patients themselves. As a result, in a given data collection, the PPG peaks that are collected from a patient will not be identical.

As a first step in analyzing the PPG waveform, it is necessary to combine multiple PPG peaks from a given patient and create a single "canonical" PPG peak that can then be used for analysis. To do this, we first identified and threw out any unsmooth peaks since the derivatives at sharp points are mathematically undefined. Such a scenario is illustrated in Figure 4.11.

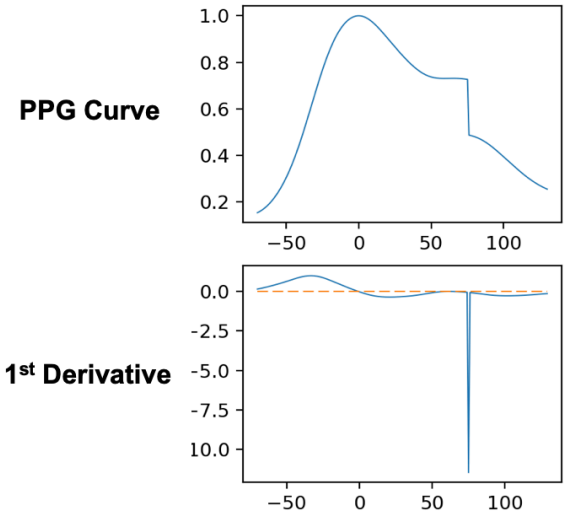

Figure 4.11: Example of an Unsmooth Peak and its Derivative

Then, we calculated the PWA Score, as described previously, of each of the remaining peaks to determine the best peaks. The resulting waveform was then constructed by averaging the four best peaks from the PPG dataset. This procedure produced a final PPG waveform array that could be used for analysis using the PWA features described above.

In Chapter 8, I present some testing and validation results for the PWA Score, based on certain clinical studies our group has done.

4.6 Measurement Scenario and Use Case

Figure 4.12 illustrates a storyboard of a potential use case for this screening tool. A community health worker would carry the mobile phone with him/her and visit each household in the area. Each member of the household would be asked to sit in an upright position at a table, and place their hand, palm facing upwards, on the table or any other flat surface. The health worker would then launch the mobile app, input patient profile information, and place the phone

on the patient's index finger, ensuring that the fingertip covers the camera and the flashlight. After completing the measurement, the health worker would then upload the measurement to our remote server, and queue a server analysis task. Once the server finishes running the PWA algorithm, it returns the results for view on the mobile phone. The results include a numerical score and some explanatory text for the patient. The mobile app are server software components are further described in detail in Chapters 6 and 7.

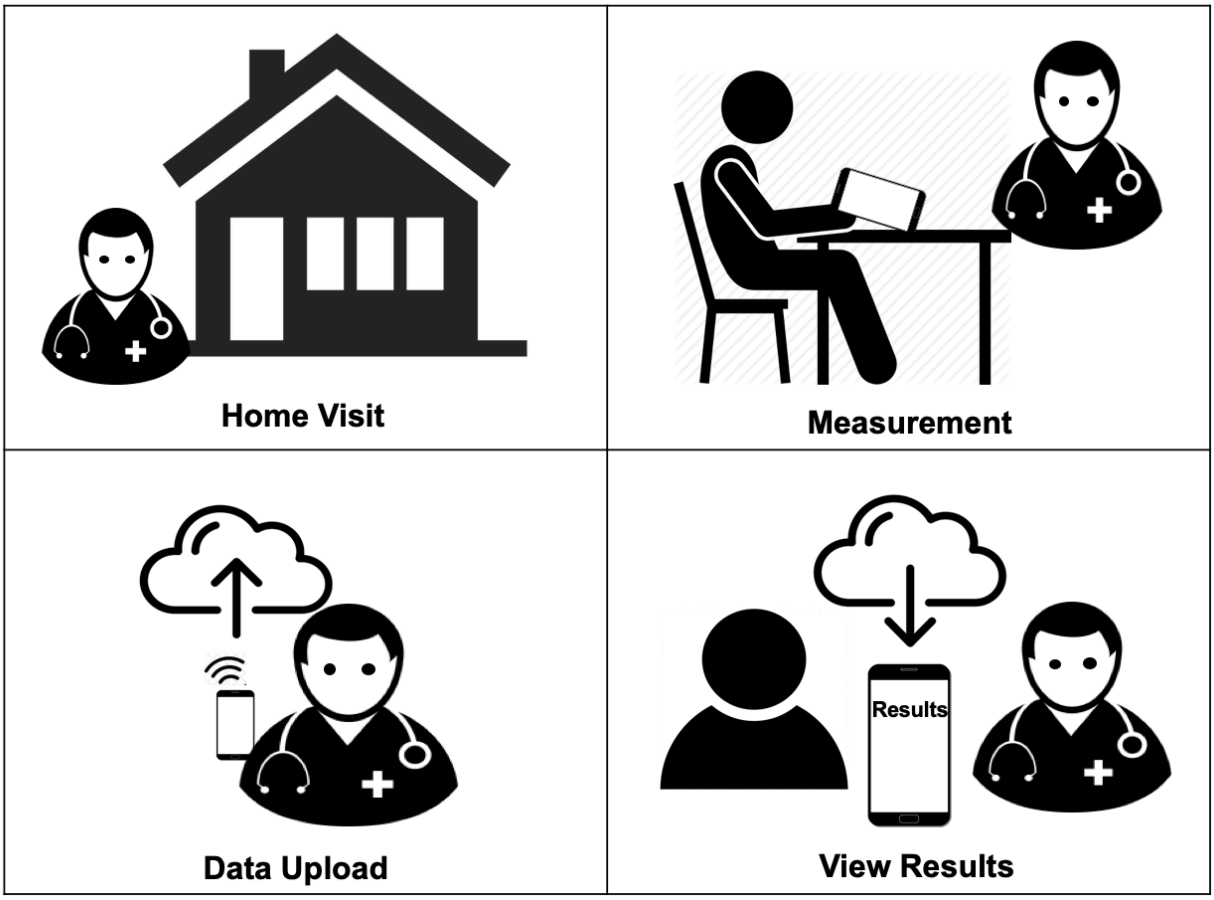

Figure 4.12: Smartphone Camera PPG and PWA Measurement Scenario

4.7 Summary

In this chapter, I discussed PWA in detail, starting with the characteristics of PPG waveforms, and then describing the two features we chose to analyze: the Rising Edge Parameter and the S-D Parameter. Although these two features can be analyzed separately using a binary classifier, to derive a continuous figure of merit parameter, we defined the PWA Score as a summation of the Rising Edge Parameter and the S-D Parameter. We performed clinical studies to validate these algorithms, which will be discussed in Chapter 8. In the next chapter, I will present PWV in detail and our methodologies.

Chapter 5

Pulse Wave Velocity (PWV)

5.1 Fundamentals of PWV

Pulse wave velocity (PWV) is a measure of the rate at which pressure waves travel through blood vessels, and is directly correlated with arterial stiffness. The fundamental principle behind measuring PWV is to measure the difference in pulse timing at two points along an arterial vessel, known as the pulse time transit (PTT), and then dividing the distance between these two points by the PTT. In the following sections, we will discuss how different types of arteries affect PWV, and traditional methods of measuring PWV. Then, we elaborate on the tools and algorithms that have been developed in our group.

5.1.1. Aortic vs Brachial PWV

Pulse wave velocity has become an effective, non-invasive way to measure arterial stiffness over the past 20 years. A higher PWV is an indication of a stiffer artery, which corresponds to an increased CVD risk [41]. However, it is important to take into account the nature of different arteries in the human body when assessing atherosclerosis and CAD.

The human body contains two major types of arteries: central elastic arteries like the aorta, and peripheral muscular arteries like the brachia. Elastic arteries, which are thinner, are more sensitive to changes in arterial stiffness as they are subject to large changes in pressure and volume throughout the cardiovascular process. Muscular arteries on the other hand are thicker, less elastic, and only need to contract or dilate when delivering blood, making them less subject to changes in pressure and volume. In 2002, O'Rourke et al. showed the changes in aortic and brachial PWV in relation to age [42]. Their results are shown in Figure 5.1. As age increases, the aortic PWV increases, while brachial PWV remains mostly unchanged.

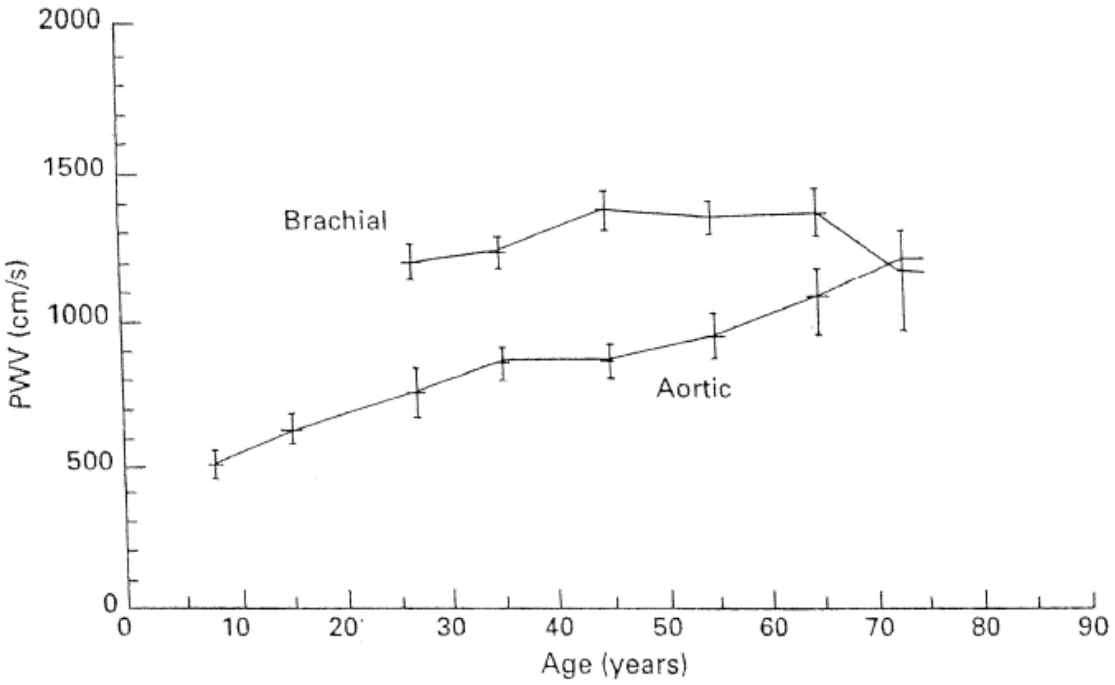

Figure 5.1: Comparison of Aortic vs Brachial PWV Changes with Age [42]

With this knowledge, we expect that the atherosclerosis and CAD disease process might be different for the central arteries versus the muscular arteries. When PWV is used as a clinical measure, PWV of a central artery should be used, such as aortic PWV – we cannot depend on

muscular PWV as an indicator of the extent of atherosclerosis progression. This distinction had to be considered when designing our screening tool.

5.1.2 Traditional Tools for Measuring PWV

Standard clinical methods of measuring aortic PWV employ inflatable cuff transducers, tonometry, or Doppler ultrasound probes. SphygmoCor is one of the leading technologies for assessing aortic stiffness non-invasively. The device calculates carotid-femoral PWV, from which aortic stiffness is approximated, using a cuff for the femoral waveform and a tonometer for the carotid waveform [43]. The Complior device also measures PWV, but instead uses up to four piezoelectric sensors for the carotid, femoral, radial, and distal locations. Additionally, Calabia et al. were able to measure PWV using a 2-D Doppler sensor and obtain numbers comparable to those from the Complior device [44]. Figures 5.2 and 5.3 show the SphygmoCor device and Complior device respectively.

Figure 5.2: Example use of the SphygmoCor [45]

Figure 5.3: The Complior Device [46]

Lower cost portable methods are also now possible using PPG, along with ECG as a timing reference. In 2000, Allen used PPG probes to measure pulse arrival times at multiple sites (ear, finger, and toe) and then used ECG to identify the time at which the heart transmitted the pulse [47]. Nitzan et al. also performed a similar study with similar findings [48]. In 2001, Mitchell et al. patented a Pulse Wave Velocity Measuring Device that used PPG and ECG to determine PWV [49].

5.2 PWV Tools from the MIT Mobile Technology Group

Many of the traditional tools discussed above are inaccessible due to their cost. For instance an ECG, while common and convenient in a hospital setting, adds additional cost and complex wiring to PWV measurements. Another issue with an ECG signal is that the timing delay between the R-wave and the detection of the pulse at the distal site includes a variable delay known as the Pre-ejection Period (PEP). The PEP is the small time delay between the ECG R-wave and the contraction of the heart muscle that ejects blood from the heart. The PEP time is also dependent on the level of sympathetic nervous system activation [50]. This variance could cause inaccuracies when calculating PWV. Because of this, other time references could be used

instead of ECG, for example a PPG signal measured at a location near the heart that can then be corrected to account for the small propagation time.

5.2.1 Design Concept

We have developed a device, called the NAJA, named after the three-headed snake in Indian mythology, that uses multi-site PPG to measure PTT and calculate PWV. The PPG signal measured from the earlobe was chosen as our reference time signal in place of ECG. Because the earlobe is close the heart and readily accessible, it is a good location for a reference timing point. Because the central and peripheral arteries have different values of PWV, we wanted to measure them separately. However, it was not practical to isolate the central artery, as that would require that a probe be placed in the patient's groin area at the femoral artery. For this reason, the patient's toe was chosen instead.

Figure 5.4 illustrates the two arterial pathways that were chosen for our design. The Ear-Finger pathway (PWV_{EF}) measures PWV in the muscular arteries, and the Ear-Toe pathway (PWV_{ET}) measures PWV in both the muscular artery along the leg and the central artery.

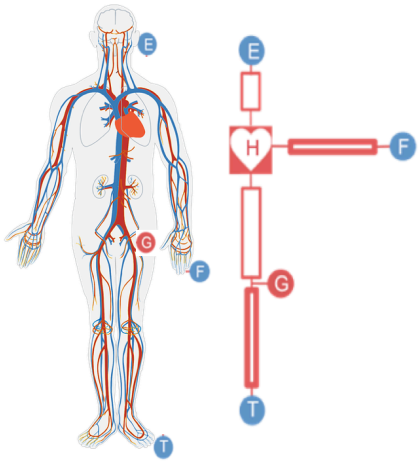

Figure 5.4: Model of the Circulatory System and PPG Probe Locations

5.2.2 NAJA Device Hardware

The components of the overall measurement hardware are a master controller unit, three peripheral PPG probes, and the mobile phone, shown in Figure 5.5. The power for all the electronics comes from the phone itself, without any external batteries needed.

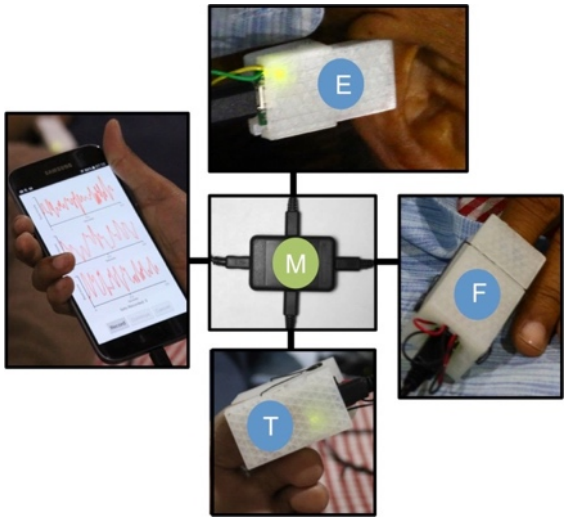

Figure 5.5: Photographs of PWV Platform including Peripheral Probes, Master Controller Unit, and Mobile Phone

The three peripheral PPG probes were custom made for the ear, finger, and toe. The PPG circuit board for each probe consists of a programmable gain (PGA) op-amp photodiode circuit, and two pairs of LEDs in a transmissive configuration. The brightness of each LED can be digitally adjusted using an Atmel ATXMega microcontroller containing a dual DAC module, which also enables the mobile app to digitally adjust the gain of the PGA. This level of customization is vital because the pulse waveform measurements at each body location require significantly different settings of brightness and gain. Additionally, differences in patient and external environment can require these settings to be adjusted as well.

The master controller unit digitally samples the analog PPG signal from each probe, and passes the sampled data to the mobile phone. Analog form signals are used in transmission to

achieve faster throughput. An Atmel ATXMega256A4U digitizes the three analog waveforms using internal 12-bit ADC modules and generates a time stamp for each set of samples with 10 µsec precision. The data as a serial data stream is then transmitted to the phone via a USB virtual COM port running at 260 kbaud.

5.2.3 Mobile Phone Software

A mobile phone software application for custom data collection was developed using the Android Java SDK. Real-time numerical processing and signal filtering was implemented in C using the Android Native Development Kit (NDK). Figure 5.6 contains screenshots of the app with anthropometric measurements and sample streaming data from all three probes. The app is discussed in further detail in Chapter 6.

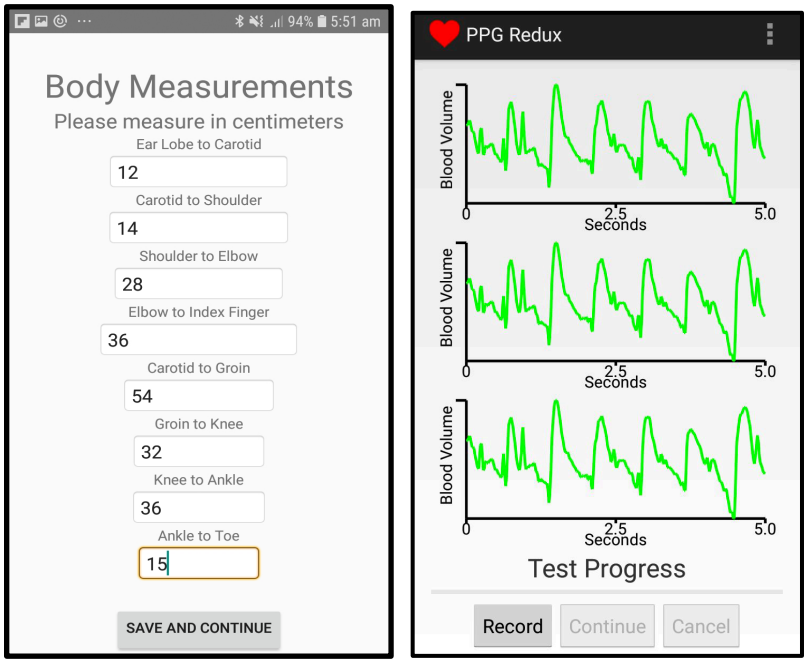

Figure 5.6: Screenshots of Custom Android Mobile Application used for NAJA Device

5.2.4 Signal Processing and Analysis

For our current system the data files are automatically uploaded via a server API to a remote server for analysis, and a process ID is created and sent to the phone. Once analysis is complete, the phone is able to query the server with the process ID, which yields a response with the result. At the time of our clinical study, the data files were manually transferred to a laptop with the analysis software installed.

The data analysis software was implemented in Python. The signal-processing pipeline involves resampling the data to 1 KHz, and then applying a mild low-pass FIR to the data. Because the individual pulse peak shape can vary for different patients, and is also a function of each patient's cardiovascular condition, the tip of the peak is not used in pulse delay calculation. Instead, the leading edge or foot of the peak is used to derive the time stamp for each peak. The 'Intersecting Tangent Algorithm' used for peak position detection is illustrated in Figure 5.7. Point A is the minimum point in the pulse trough, Point B is the point of maximal upstroke, and Point C is the intersection of the horizontal and tangent lines from A and B respectively. Point C is taken as the arrival time of a given pulse.

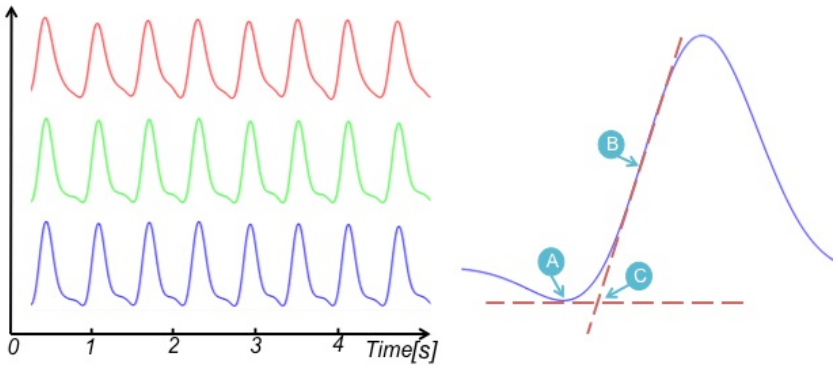

Figure 5.7: (Left) Sample Synchronized PPG Signals from Ear (red), Finger (green), Toe (blue). (Right) Illustration of Intersecting Tangent Method

A pulse wave starts at the heart, and subsequently travels to the ear, finger, and toe along the paths shown in Figure 5.4. Using the diagonal distance from the heart to the ear lobe, and the distance between the heart to the index finger and big toe, respectively, we can calculate PWV_{EF} and PWV_{ET} as shown below:

$$PWV_{EF} = (d_{heart-finger} - d_{heart-ear}) / t_{EF}$$
$$PWV_{ET} = (d_{heart-toe} - d_{heart-ear}) / t_{ET}$$

5.3 Measurement Scenario and Use Case

Unlike the PWA screening tool, which can be implemented by a health worker with only a mobile phone, the PWV measurement is designed to be used at a primary care health facility. Figure 5.8 illustrates a story board of a potential use case for the NAJA PWV screening tool. In this case, since obtaining accurate body measurements and finding the patient's pulse requires some level of basic medical training, a trained nurse or GP doctor would carry the mobile phone, the NAJA device, and a measuring tape with him/her and visit each patient in a primary health clinic in low-resource areas.

Each patient would be asked to lie flat on a bed for screening. The nurse/doctor would start by launching the mobile app and inputting patient profile information. Then, he/she would take the required body measurements by hand using a measuring tape, and input the values to the mobile app. Afterwards, the nurse/doctor would clip the three probes to the patient's ear lobe, index finger, and big toe, and record a stable 30-second measurement. After completing the measurement, he/she would then upload the measurement file to our remote server, and queue a server analysis task. Once the server finishes running the PWV algorithm, it returns the results for view on the mobile phone. The results include numerical values corresponding to PWV and

PTT and some explanatory text for the patient. The mobile app and server software components are further described in detail in Chapters 6 and 7.

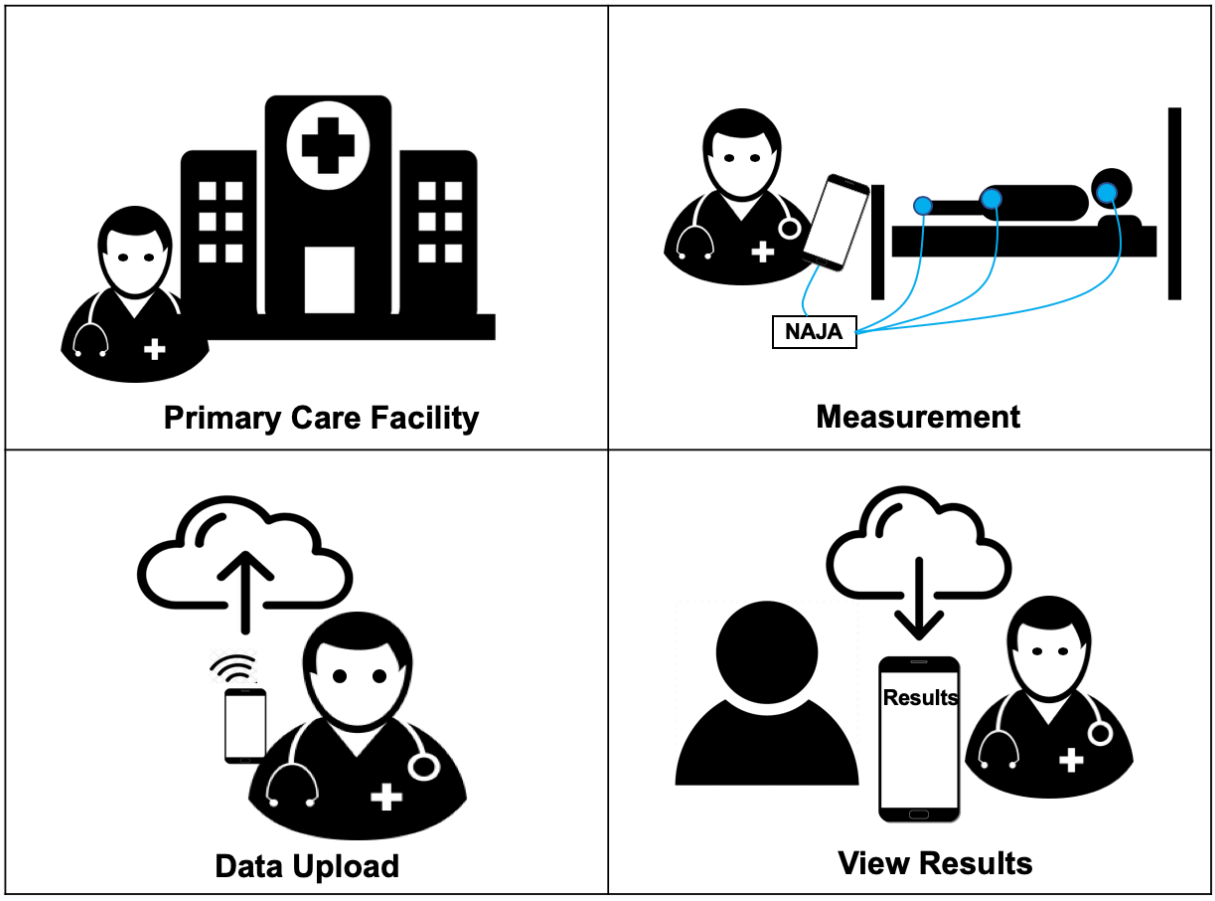

Figure 5.8: NAJA Device and PWV Measurement Scenario

5.4 Summary

In this chapter, I discussed PWV in detail, starting with the difference between aortic and brachial PWV, and traditional methods of measurement. Instead of using an external cuff transducer, tonometry, or Doppler methods, we have chosen to use PPG. Though PPG has been used before in conjunction with ECG as a timing reference to measure PWV, we developed the NAJA device that uses a third PPG signal from the ear as a timing reference, eliminating the

extra cost and complexity added by ECG. After describing the hardware and software implementations in detail, I highlight a potential use case for this tool. In the next chapter, I detail the mobile apps used in our screening platform.

Chapter 6

Android Mobile App Implementation

This chapter discusses the set of mobile applications integrated in our CVD screening platform. The Android applications used to collect measurements were initially standalone applications that were built by previous students in the group. The applications were developed specifically for data collection using the Android JAVA SDK. Real-time numerical processing and signal filtering is implemented in C using the Android Native Development Kit (NDK). These mobile apps have been tested and used on a variety of Android devices including a high-end phone (Samsung Galaxy S7), a tablet (Samsung Galaxy Tab 3), and a lower-cost phone (Samsung Galaxy J7 and J8).

To integrate them as part of a complete set and with the server, these applications were updated to be compatible with the most recent version of Android. They also now include PyMedServer-Android, Android libraries that were also created as part of John Mofor's master's thesis [33]. These libraries provide a template that all of our mobile applications follow, but customizations were made on top of them to address the specific CVD screening platform needs.

6.1 Android Libraries

Figure 6.1 illustrates an architectural diagram of the Android mobile app components. The two standard libraries in PyMedServer-Android are APILib and StorageLib. Each custom measurement app contains a standard landing page for clinician login and patient selection that is included in StorageLib. Once a patient to screen is selected, the application continues prompting through its specific set of screening activities. Then, the results are saved locally on the mobile phone and can be uploaded to the server. StorageLib was customized to support database models for CVD questionnaire, PWA, and PWV measurements specifically. Once the measurement is saved, APILib enables communication with the server. It prepares the data in JSON format that the server can interpret, and makes HTTP API calls to upload measurements, download measurements, and run analyses. APILib and StorageLib also contain built-in functionalities for authentication and offline support.

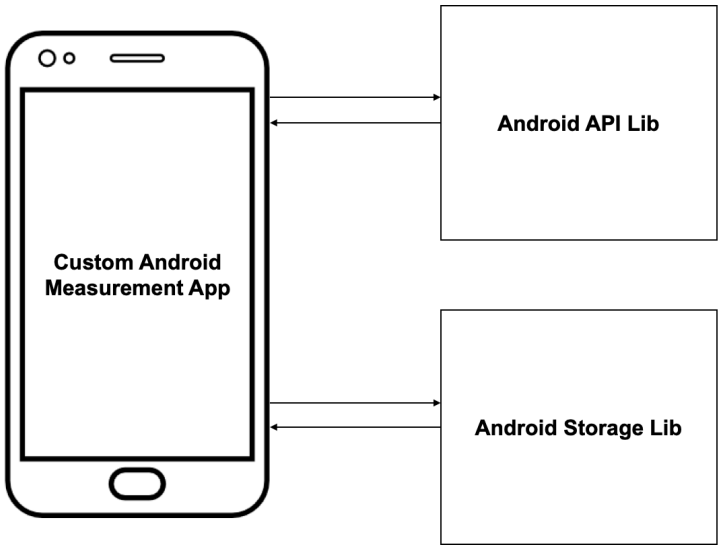

Figure 6.1: Custom Android Measurement App Architecture

6.2 Mobile Applications for Measurements

We have integrated three mobile applications for measurements: a CVD questionnaire application, the PWA application that uses the smartphone camera to record finger PPG measurements, and the PWV application for the external NAJA device. Each of the applications can be used on their own for recording and labeling measurements, or launched from the container application, which is discussed in Section 6.3. All measurements can be uploaded to the server and deleted locally on the phone. There is also the option to sync the phone with the server to obtain any measurements that exist on the server, but are not on the phone.

6.2.1 CVD Questionnaire App

The CVD questionnaire app asks the user to fill out a series of questions based on the Framingham Risk Score model. These questions include a patient's cholesterol levels, blood pressure, smoking status, diabetes diagnosis, and medication information. Using the inputted values, the app then calculates an overall risk score using the Framingham Risk Score model and displays the results. Since this is a simple arithmetic calculation, it can be done as a local analysis on the phone, without needing to invoke the server. The measurement is then saved locally and can be uploaded to the server. Figure 6.2 shows sample screenshots of the CVD questionnaire app.

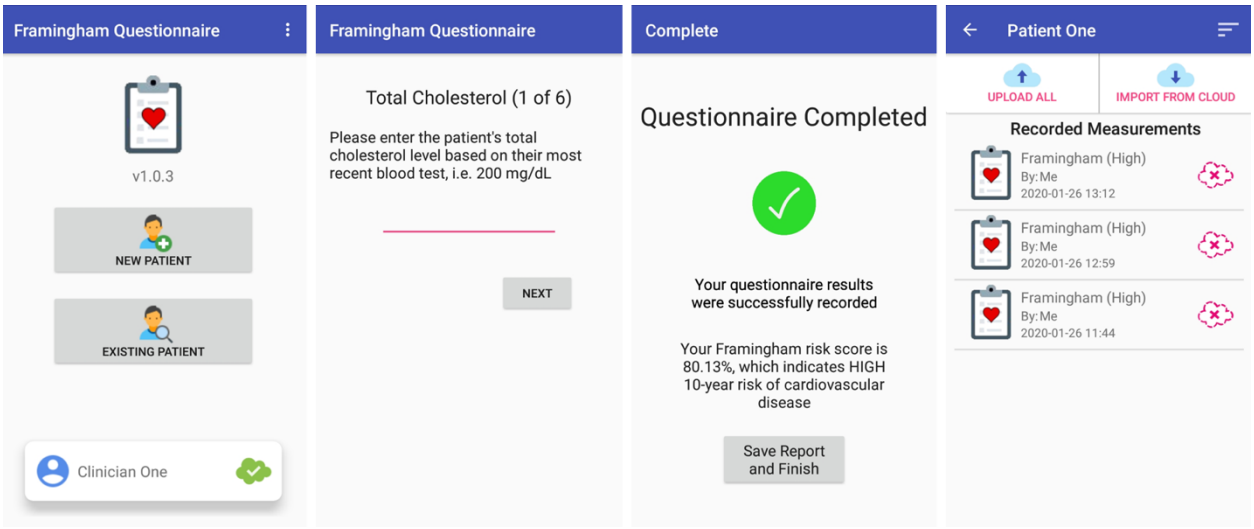

Figure 6.2: Sample Screen Captures of CVD Questionnaire Mobile App

6.2.2 Smartphone Camera PPG App

The smartphone-based finger PPG app uses the phone's camera to record a time series measurement of a patient's pulse waveform. The patient is instructed to rest their hand, facing palm upwards, on a flat surface. The phone's camera is then placed on the patient's index finger so that it covers both the camera lens and the flash light. Once a stable pulse is detected, the app records a 30-second measurement of the pulse waveform, and stores it locally on the phone. The user then has the option to upload the measurement to the server. Figure 6.3 shows sample screenshots of the camera PPG app.

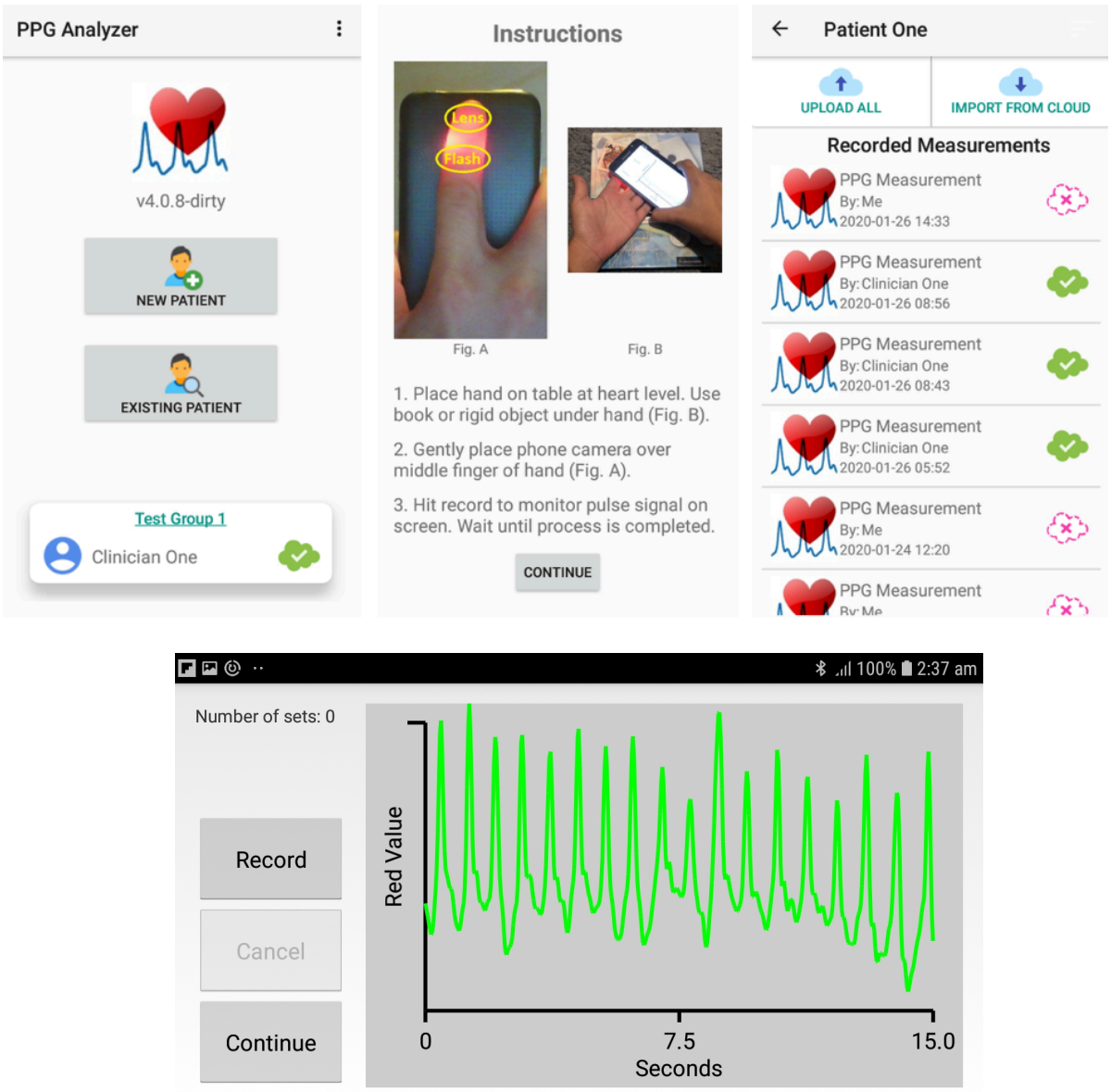

Figure 6.3: Sample Screen Captures of Mobile App for Camera Finger PPG

6.2.3 PWV App for NAJA Device

The NAJA device is intended to be plugged in to a mobile phone and used with the PWV app. First, the patient is asked to lie flat on their back patient's anthropometric measurements are taken by hand and recorded in the app. Then, the three probes of the NAJA device are clipped

onto a patient's ear, finger, and toe, all on the same side of the body. Once stable pulse waveforms are detected, the user records a 30-second measurement, which is then stored locally and can be uploaded to the server. Figure 6.4 shows sample screenshots of the PWV app.

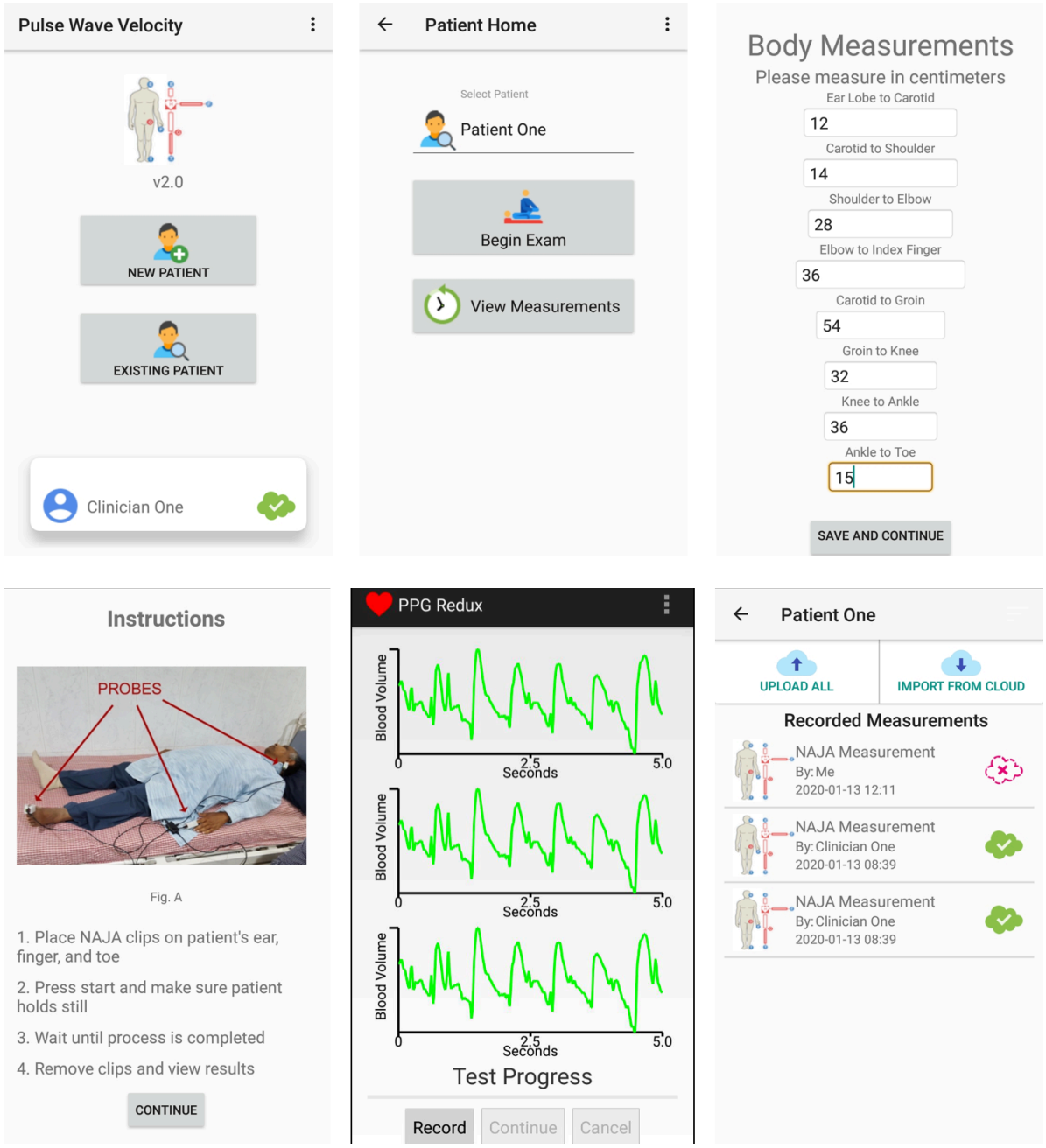

Figure 6.4: Sample Screen Captures of Mobile App for NAJA Multi-Site PPG

6.3 Measurement Integration

To integrate all the standalone measurement applications, we created a “container app”. Similar to all the measurement apps, the container app also has the standard landing page, user authentication, and patient selection features. Through this app, when users choose to begin the exam, the start buttons next to each type of measurement will launch their corresponding measurement applications. If the measurement applications have not been downloaded, the user will be redirected to the exact page in the Google Play Store to download the application.

Once a measurement is successfully recorded, the corresponding start button will display as green, indicating that that measurement is complete. Measurements are saved locally on the mobile phone and can be uploaded to the cloud when there is internet connectivity. The cloud icon next to recorded measurements indicate whether the measurement has been uploaded or not. The container application also has functionality to run computer analysis on the server and view results, which the individual measurement applications do not have. When choosing to run a new computer analysis, the user is prompted to select which measurements to use for the analysis. Once analysis is complete, an HTML web view containing the results is returned to the mobile phone for display. Measurements and analyses that were previously saved to the cloud, but do not exist on the current mobile device can also be imported and synced. Figure 6.5 shows some sample screenshots of the container app.

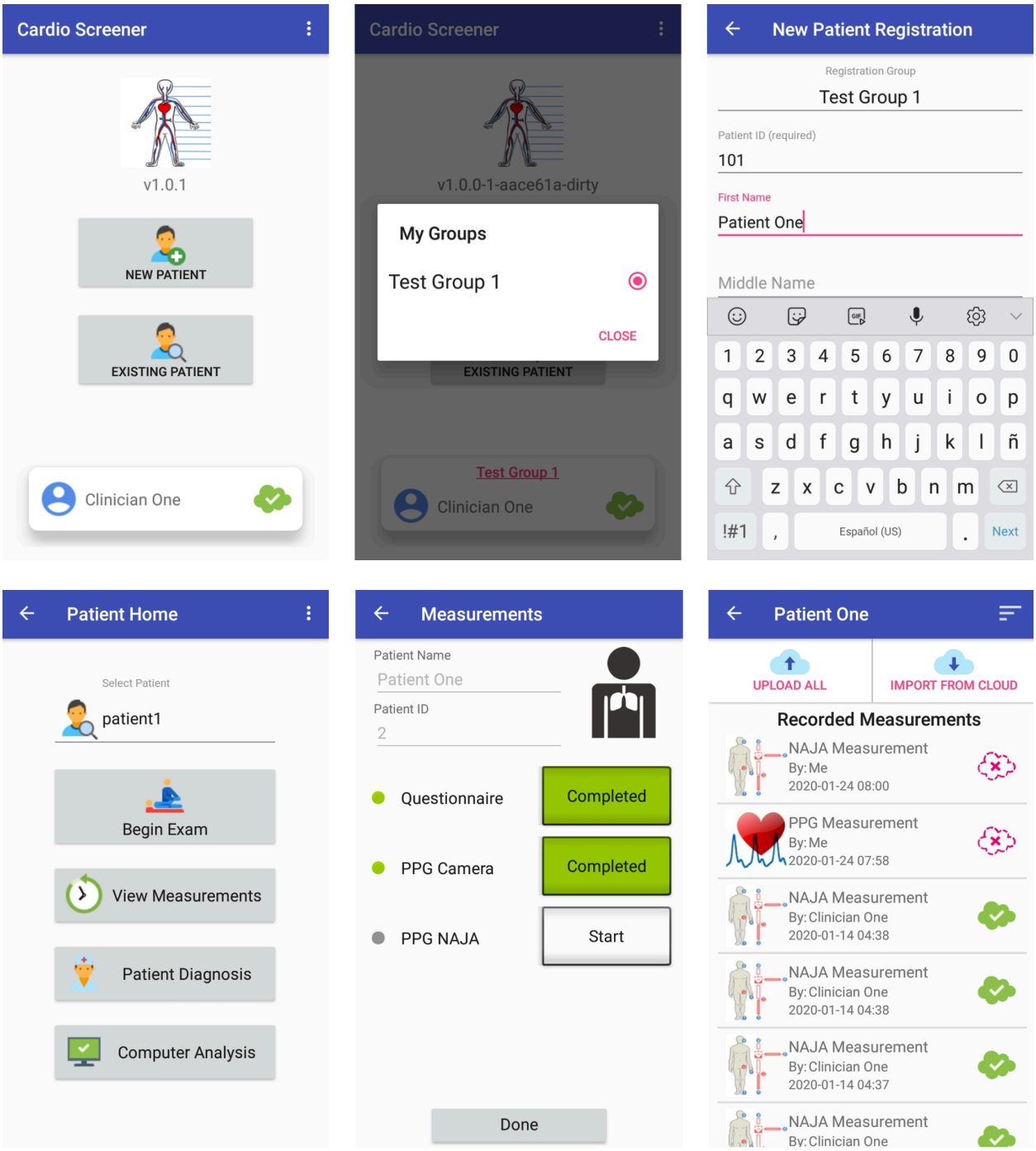

Figure 6.5: Sample Screen Captures of CVD Container App

6.4 Summary

In this chapter, I described the individual measurement mobile apps, their integration with the PyMedServer-Android libraries, as well as integration with the container app. I also briefly introduced communication between the apps and the server. In the next chapter, I discuss in detail the server infrastructure, customizations, database models, and API formats.

Chapter 7

Server Platform

In this chapter, we describe the implementation of the CVD server platform, which stores all of the recorded measurements and runs our analysis algorithms. The CVD server provides a way to record and upload data to cloud storage through the Android mobile application, and then sync and view the data on any Android mobile device or tablet. This platform is essential for the integration and scalability of our screening tools.

7.1 Server Architecture Overview

7.1.1 Background

The server architecture used for the CVD server was developed by a previous M.Eng. student in our group, John Mofor, as a separate master's thesis. He developed PyMedServer, a server framework built on Django, that allows for large scale collection of medical data. The framework is easy to use and maintain, and supports a rich set of functionalities that are common to all of our group's projects such as Mobile Client Support, User Authentication and Authorization, Permission Classes, and support for Asynchronous Tasks, and other useful features [33].

Figure 7.1 illustrates a block diagram of the server architecture. The smartphone clients send collected data to the server, which first goes through the load balancer. The load balancer handles all tasks that do not require a Django backend, since Django backends are limited resources and we do not want to be overloading them. All remaining tasks that cannot be handled by the load balancer are sent to a Django backend. Time and calculation intensive processes such as machine learning are handled by the background job runner to relieve burden on the Django backends, but this does not have direct access to the clients. All data and results are stored in the database, from which clients can pull saved measurements and analyses.

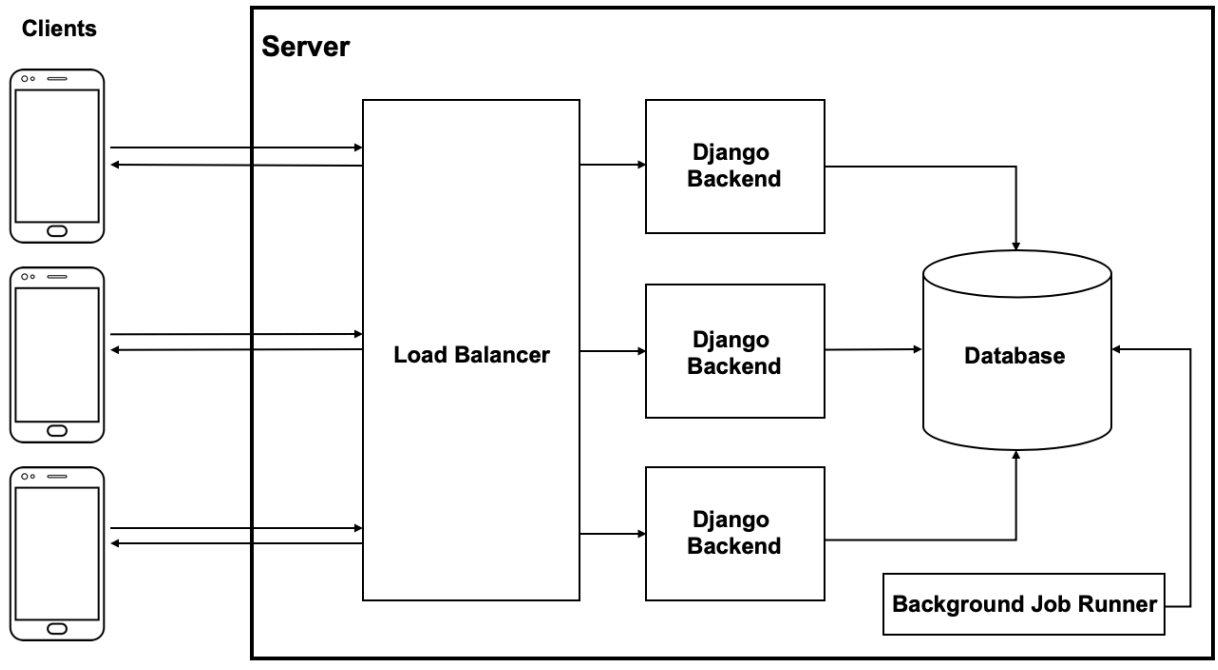

Figure 7.1 High-level Server Architecture Overview

In this project, the PyMedServer framework was customized to support the needs of our CVD screening platform. Custom APIs were developed to support adding and viewing measurements, clinician diagnoses, and server analysis. First, we will describe the general database and API structure supported by PyMedServer. Then, we will go into detail about how we used it to create the backend server APIs called by the Android mobile applications.

7.1.2 General API Design

To make future development and maintenance of the server and mobile applications easier, we adopted the same format of API calls across all of our group's projects. The API structure was developed by Shivani Chauhan, M.Eng., as part a separate master's thesis for our group's diabetes project [51]. In general, when PyMedServer receives an HTTP or HTTPs request, it matches the URL to a class-based view that processes the request and returns a response. Specifically, we use an APIView class from the Django REST Framework library. An incoming request is dispatched to an appropriate handler method such as .get(), .post(), or .delete() [52]. The request is parsed and sent to a request serializer, which is used to convert the data sent from the HTTP request to native Django objects [53]. A response serializer is used to convert a Django object to an HTTP response.

7.1.3 Server Database

PyMedServer is set up to install and configure a PostgreSQL database automatically. The default Django database features used represent database objects as Python classes called models. Each model has a list of attributes that represent database fields [54]. Django provides an automatically-generated database-access API that is used to create, retrieve, update, and delete

objects [55]. In the CVD server, we use fields of type Integer, Float, Boolean, String, and FileField to store information from the uploaded measurements. Additional field types are used to organize the model structure of the database. All objects stored in the database are associated with a unique ID.

7.1.4 User Management

Our CVD screening platform is intended to be used by several different types of users such as clinicians, health workers and nurses, and patients. Users in these separate classes have different sets of privileges and access levels. PyMedServer has a user management system that creates different User Groups that contain all of the users in a same study. A user can belong to multiple User Groups since they can be part of multiple studies. The three classifications of users are either Patient, Clinician, or Clinician Admin. Patients are only authorized to view their own test results. Clinicians and Admins are able to register patients, take measurements, and provide clinical diagnoses. Admins have an additional set of privileges, which include approving other clinician registration requests and adding them to User Groups. PyMedServer provides these permission classes to manage the different access levels of each user type.

7.2 Creating New Measurements

For the scope of this thesis, we focus specifically on the questionnaire and PPG measurements discussed in Chapter 3. The measurements are added by a set of Android mobile applications, which is discussed further in Chapter 5. The user records the measurements using a mobile phone, which uploads them to the server and stores the server responses back to the

application. This section describes the implementation of the Add Measurement API which is used to upload measurements to the server.

7.2.1 Measurement Database Model

Measurements uploaded to the server are stored as models in the database, which store information from the measurements as fields. For the questionnaire, the database fields contain the answers to the questions such as height, weight, blood pressure, smoking frequency, diabetes diagnosis, and medications. The PPG measurements include pulse wave analysis (PWA) using the phone camera, and pulse wave velocity (PWV) using external probes. For both of these measurements, the model contains a database FileField corresponding to the time series CSV file.

Additionally, for each measurement object, a corresponding metadata model called DiagnosticMeasurementMetaData is also created and stored in the database. The metadata model stores information about the measurement itself such as which patient the measurement belongs to, and the time and location the measurement was recorded. Together, the measurement and metadata are stored under one object called DiagnosticMeasurement. This object includes fields that correspond to all of the different possible measurements that can be taken, but only the field for one measurement and metadata will ever be populated, leaving the remaining others null. Figure 7.2 visualizes an example DiagnosticMeasurement containing a CardioQuestionnaire and its DiagnosticMeasurementMetaData. In this example, pwa_measurement and pwv_measurement, the remaining fields in DiagnosticMeasurement, are null.

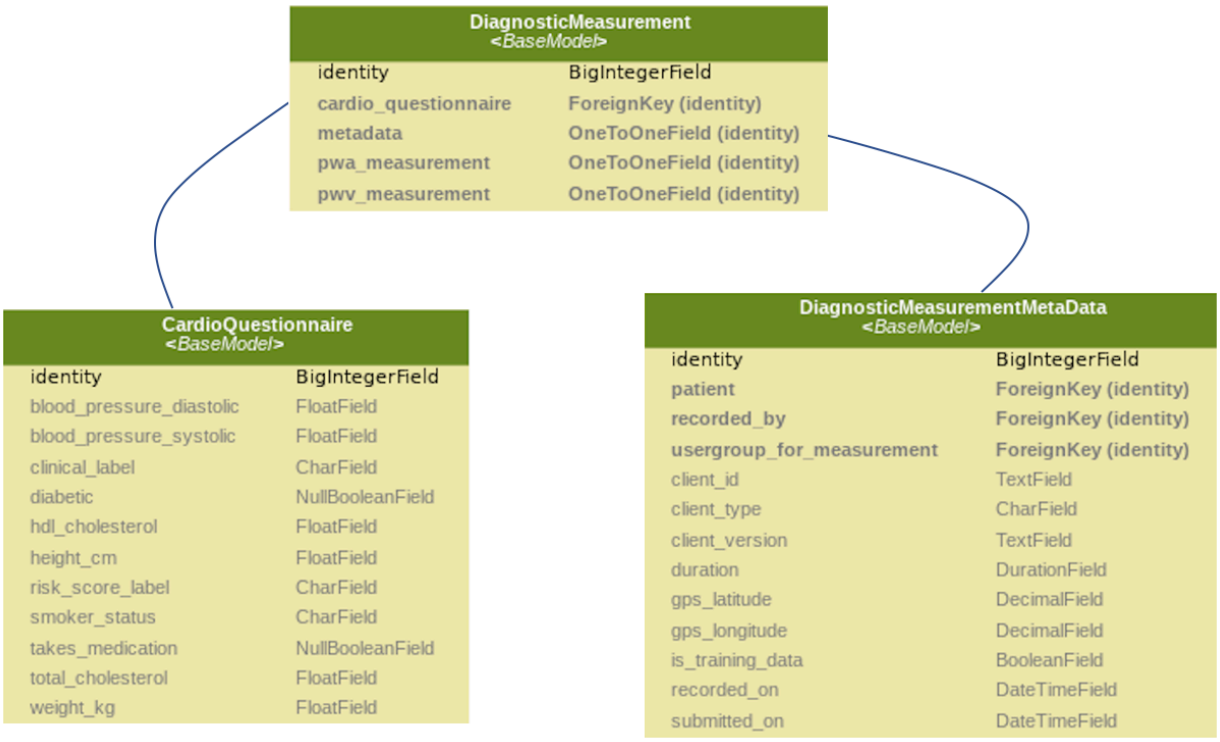

Figure 7.2: DiagnosticMeasurement Object Containing CardioQuestionnaire and DiagnosticMeasurementMetaData

7.2.2 Add Measurement API

The Add Measurement APIs follow a format that is uniform across all of our group's servers, and are exclusively called by the mobile applications. The application sends an HTTP request with JSON data formatted as the DiagnosticMeasurement object that will be stored in the database. If the measurement being sent is a questionnaire, the JSON request would contain the metadata along with the questionnaire responses. If the measurement is either a PWA or PWV recording, the JSON request would contain the metadata and an encoded CSV file corresponding to the time series recording.

For each measurement type, there is a specific URL that must be called to add that measurement. These URLs are listed below:

1. https://healthyheart.dev/apis/diagnostics/add_measurement/questionnaire/clinician/
2. https://healthyheart.dev/apis/diagnostics/add_measurement/pwa/clinician/
3. https://healthyheart.dev/apis/diagnostics/add_measurement/pwv/clinician/

For future server development, all additional measurement types will follow the same URL format.

All Add Measurement requests are POST requests. Once the URL is called, the reverse lookup finds the APIView associated with that URL and the request is dispatched to the post handler. The request serializer then converts the parsed data into a Django object. The model is validated to ensure that the request has all of the necessary fields in order to be saved as a DiagnosticMeasurement object in the database. If any required field is missing, the model will fail to validate. If the model validates, then the metadata, measurement data, and overall measurement object is saved to the database. A response serializer converts the final DiagnosticMeasurement object into an HTTP response that is returned back to the mobile application.

7.3 Server Analysis Algorithms

To integrate the algorithms used to extract PWA features from pulse waveforms, to calculate PWV, and for machine learning, they must be supported by the server. This feature enables scalability of our CVD screening platform. Prior to server integration, all pulse data was collected and stored locally on mobile phones and then manually extracted onto a laptop for processing since the mobile phones were not powerful enough to handle the computationally intensive algorithms. This method did not scale well, and made it difficult to maintain and keep track of the data as the number of files grew and the project was passed onto new students.

Supporting these algorithms on the server allows for server analysis to be run in real-time, and eliminates the dependency on having very powerful mobile devices.

7.3.1 Server Analysis Database Model

The server analysis is stored as a ServerDiagnosticPredictions object, which inherits from AbstractDiagnosticPredictions. This model contains the overall CVD risk prediction, PWAResult, PWVResult, and other fields such as the measurements used in the analysis, created time, and any errors encountered while running the analysis algorithms. A PWAResult contains the features extracted from the time series data file, which are the rising slope and SD parameter of the average pulse waveform. A PWVResult contains the pulse time transit calculated between ear-finger, ear-toe, and finger-toe locations. Figure 7.3 shows the model relationships.

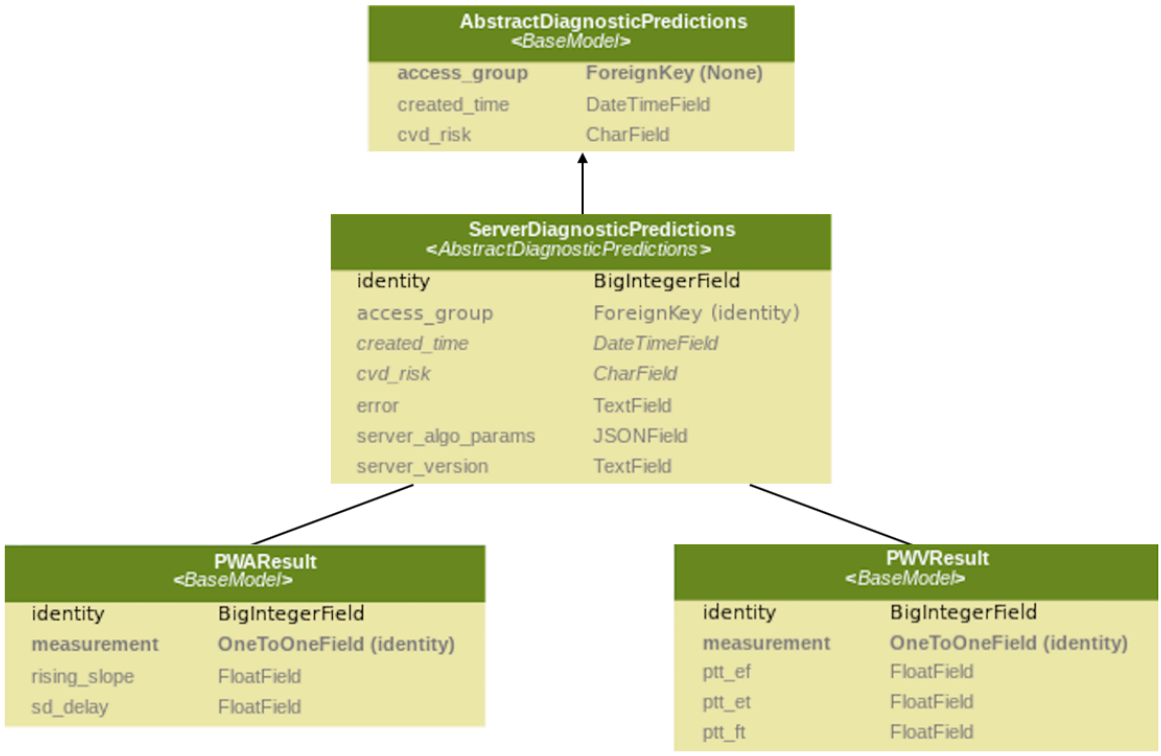

Figure 7.3: ServerDiagnosticPrediction, AbstractDiagnosticPrediction, PWAResult and PWVResult

7.3.2 Run Analysis API

The Run Analysis API is also exclusively called by the Android mobile application. It is designed such that only one Run Analysis API needs to be called to handle server requests for all types of measurements instead of having a separate API for each measurement. This simpler design allows for a more static Android mobile application when new types of measurements are introduced on the server, and is helpful for combining measurement analyses to determine a final CVD risk classification. The API is called with a JSON request that contains the measurement_ids for server analysis. The database is then accessed to find the corresponding measurement to each unique ID in measurement_ids. If the measurement already has an associated result from a previous Run Analysis call, the result will be added to the corresponding result field of the ServerDiagnosticPrediction. Otherwise, each unanalyzed measurement will kick off an asynchronous task on the server to calculate a measurement result.

7.3.3. View Measurements and Results APIs

There are three APIs for viewing measurements and results: View Measurements, View Clinician Analyses, and View Analyses. View Measurements allows the user to view the measurement details. View Clinician Analyses returns a professional diagnosis by a clinician: a ClinicianDiagnosisPrediction object. View Analyses returns a ServerDiagnosticPrediction based on the measurement IDs selected for automated server analysis. Table 7.1 shows the different request parameters and response objects for each of these APIs. The View Analyses response also returns an HTML field so that the Android application can display the analysis as a WebView that properly formats the HTML.

API	Request Parameters	Response
View Measurements	Patient IDs Measurement IDs UserGroup IDs	DiagnosticMeasurement
View Clinician Analyses	Patient ID UserGroup IDs	ClinicianDiagnosticPrediction
View Analyses	Patient IDs Measurement IDs Server Diagnosis IDs	ServerDiagnosticPrediction

Table 7.1: Request Parameters for View Measurements and Results APIs

7.4 Clinician Diagnosis and Editing Measurement Labels

The server platform supports professional clinician diagnosis of a patient. Clinicians can annotate diagnoses through the Android mobile application, which calls an Add Analysis API. This diagnosis information is stored as a ClinicanDiagnosticPrediction object. There are a set of predefined choices for the clinician to pick for most cases: healthy, abnormal, hypertension, CVD, and undetermined. In the case of uncommon diagnoses, there is also an additional free-form text field that gives flexibility in the diagnosis. Additionally, the platform allows for labelling of individual measurements through the mobile app. The predefined choices for labelling both overall diagnoses and individual measurements allow for training machine learning models.

7.5 Summary

In this chapter, I presented a high-level overview of the PyMedServer architecture, and then described the customizations made for the CVD server specifically. I discussed the database models and API structures in detail, which facilitate integration of the screening tools, centralized and secure data storage, and automated analysis algorithms. In the next chapter, I will discuss the clinical studies done to validate performance of the PWA, PWV, and machine learning algorithms.

Chapter 8

Clinical Evaluation of Pulse Wave Analysis (PWA)

In this chapter, I present an evaluation of our PWA algorithms using data from two separate clinical studies. These are described below.

8.1 Study #1: University Students

8.1.1 Study Objectives

To better understand the distinction between young healthy individuals who regularly exercise and those who do not, and to validate the PWA Score metric, I designed and conducted study at MIT and in the greater Boston area. This study was approved by the MIT IRB committee, known as COUHES, under protocol number 1911000045. PWA features were extracted from the collected data and analyzed for comparison between the two study groups.

8.1.2 Study Population

The study subjects were divided into two groups: athletic and non-athletic. Athletic subjects were defined as individuals who regularly did cardio exercise at least three times a week. Anyone who did not meet this level of routine exercise was considered non-athletic. All study members were young and healthy individuals between the ages of 18 and 25. This study population consisted of 9 athletic individuals and 10 non-athletic individuals.

8.1.3 Study Protocol

Participants were first asked to fill out a basic questionnaire regarding their amount of routine cardio exercise, and then asked to sit upright and rest their hands on a stable flat table, as shown in Figure 8.1. Then, a smartphone was placed such that the participant's index finger tip covered the camera and flashlight. Once a steady pulse was detected, the phone recorded the pulse for 30 seconds. These pulse waveforms were then plotted and analyzed using our PWA algorithms.

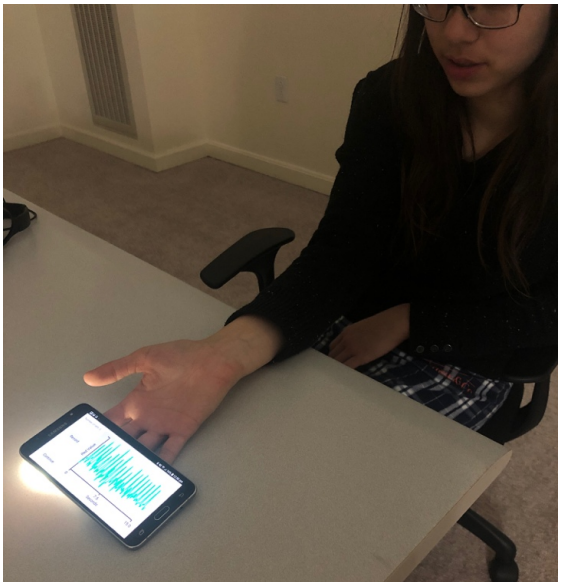

Figure 8.1: A Subject Undergoing Smartphone Camera PPG Measurement

8.2 Study #2: Indian CAD Assessment

8.2.1 Study Objectives

The objective of this study was to develop algorithms capable of characterizing any arbitrary PPG waveform. To validate the performance of the PWA Score metric on different clinical cardiovascular health classifications, I conducted, originally designed by Niccolò Pignatelli, at the Sengupta Hospital and Research Institute in Nagpur, India. Through this study, we can compare the PPG waveforms of older healthy people and CAD patients. This study was approved by both the MIT IRB committee, known as COUHES, under protocol number 1811598864, and by the IRB committee in Nagpur. PWA features were extracted from the collected data and analyzed for comparison between the two study groups in this study, and with the two groups from the study on University Students.

8.2.2 Study Population

The study subjects were divided into two groups: unhealthy and “healthy”. Unhealthy subjects were defined as patients who were either clinically diagnosed with CAD, or had strong risk factors of CAD (hypertension or diabetes). Healthy subjects were defined as age-matched controls who did not have CAD, hypertension, or diabetes. The study population consisted of 18 “healthy” subjects and 17 unhealthy subjects, all typically over the age of 40.

8.2.3 Study Protocol

Participants were first asked to lie down on a hospital bed and place their hand on a stable flat surface, such as a hardcover book, with their palm facing upwards. Then, a smartphone was

placed such that the participant's index finger tip covered the camera and flashlight. Once a steady pulse was detected, the phone recorded the pulse for 30 seconds. These pulse waveforms were then plotted and analyzed using our PWA algorithms.

8.4 Data Analysis

The raw data collected by the phone was saved as a time series CSV file. To analyze the data and extract PWA features, we first pre-processed the data by up-sampling to 1000 Hz and filtering using a low-pass filter with cutoff of 0.15 Hz and a high-pass filter with cutoff of 20 Hz to avoid filtering out anything related to the heartbeat. Figure 8.2 compares a the noisy raw signal of a sample dataset with the resulting filtered signal. Then, we apply our peak finding algorithm to identify each individual curve. Figure 8.3 shows the identified peaks and zero crossings of a sample PPG signal. After filtering out any unsmooth curves, the PWA Score was calculated for each of the remaining peaks to determine the best peaks, The best peaks were then used to construct a canonical peak that we then analyzed using the PWA features. Figure 8.4 shows the best four peaks from the sample collected signal, and the corresponding average PPG curve. This process was repeated for all pulse data collected from the study participants.

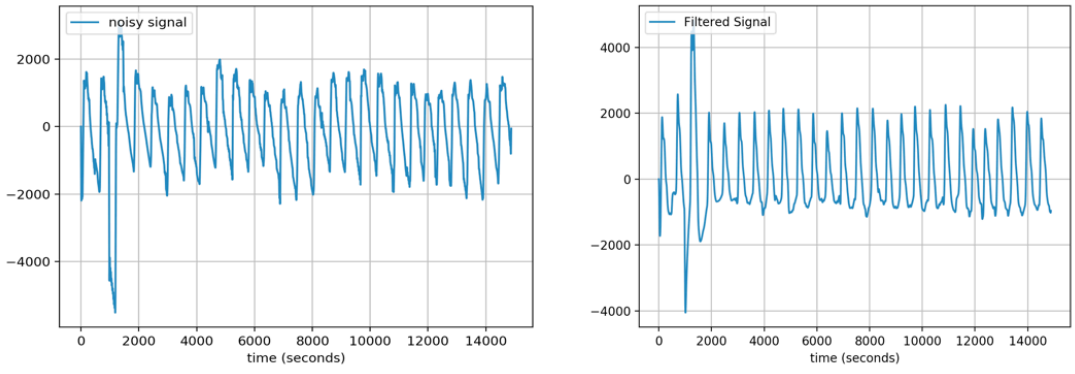

Figure 8.2: Noisy (left) vs Filtered (right) Sample PPG Data

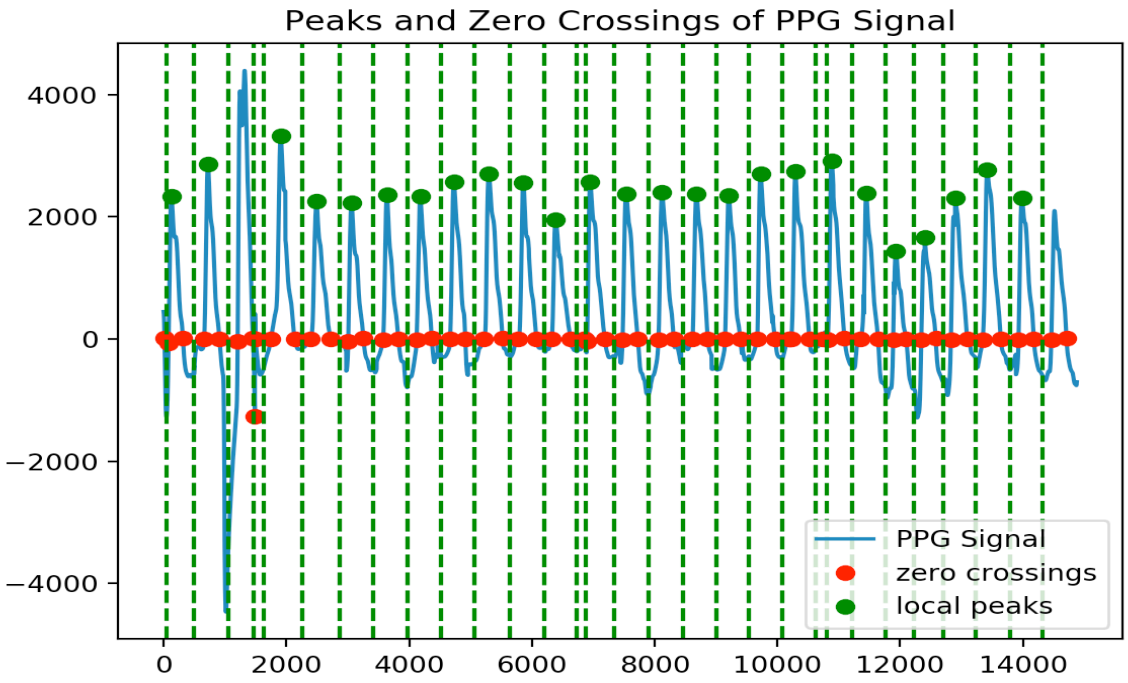

Figure 8.3: Peaks and Zero Crossings of a Sample PPG Signal

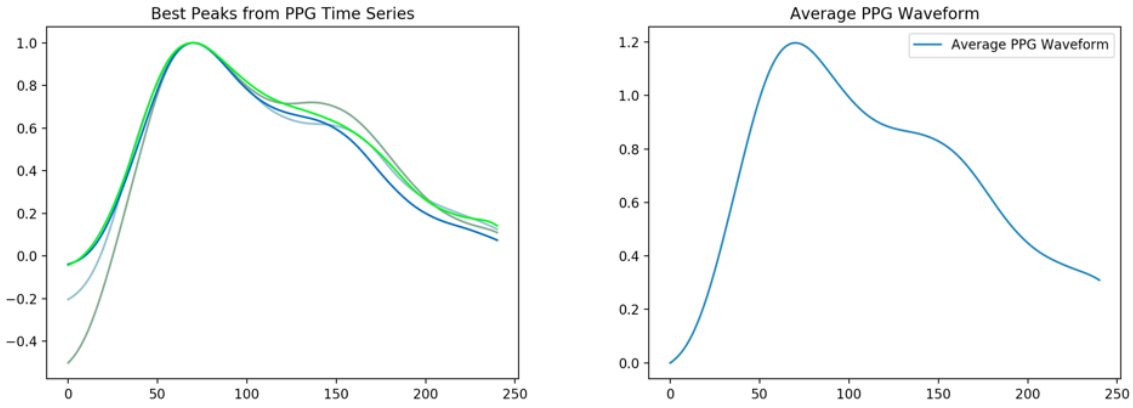

Figure 8.4: Best Peaks Scored by the S-D Parameter (left) and the Resulting Average PPG Waveform (right)

8.5 Results

The resulting canonical PPG waveforms for each participant categorized as non-athletic, athletic, old healthy, and old unhealthy, are plotted below in Figure 8.5. From theses average curves, I analyzed the Rising Edge Parameters, S-D Parameters, and aggregate PWA Scores as presented in Chapter 4. The median Rising Edge Parameters by health category are summarized in Table 8.1 and Figure 8.6. The median S-D Parameters are summarized in Table 8.2 and Figure 8.7. Finally, the median overall PWA Scores are summarized in Table 8.3 and Figure 8.8.

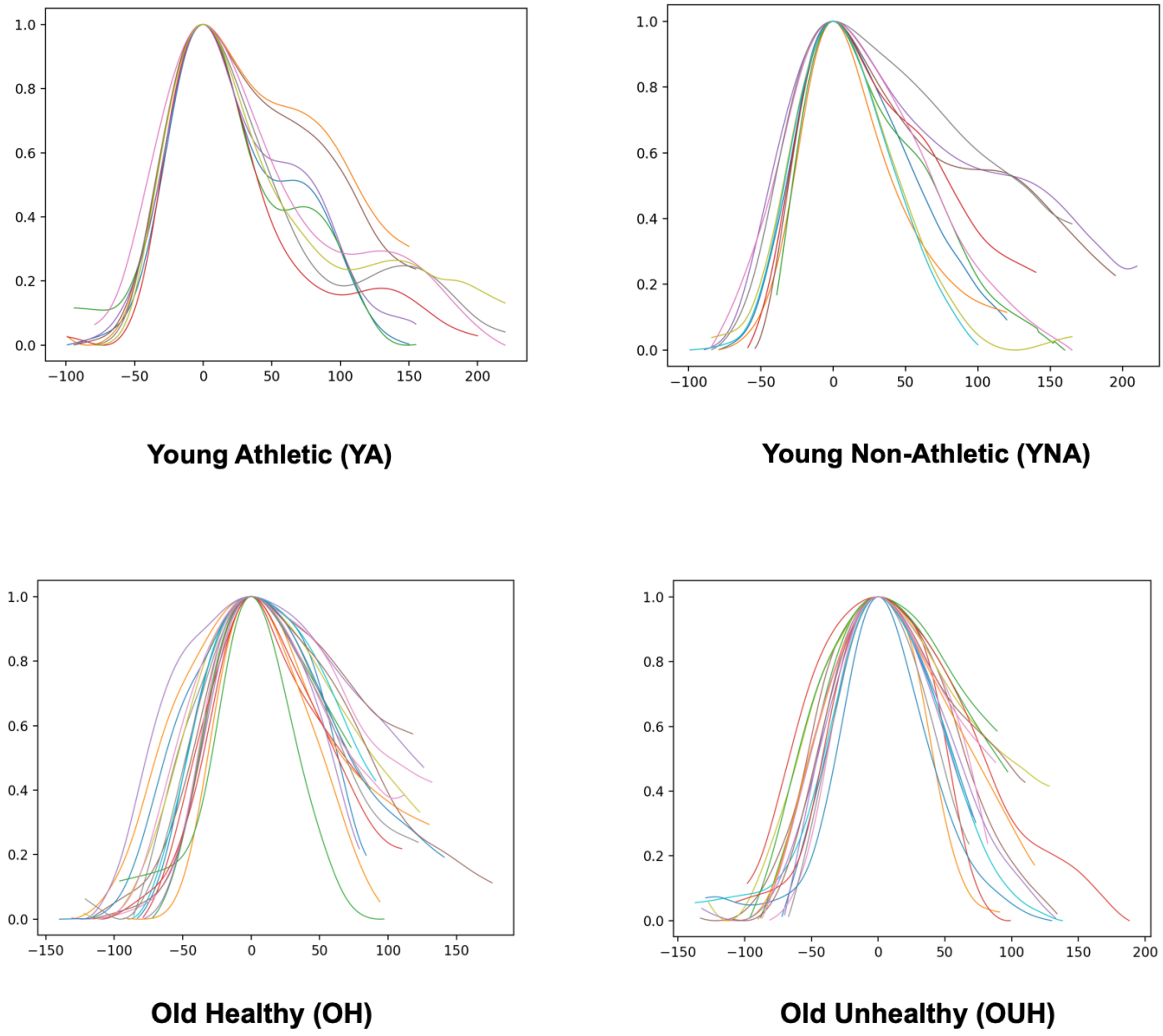

Figure 8.5: Average Pulse Waveforms by Cardiovascular Health Classification

	Median Rising Slope (Std. Dev.)	Median Rising Edge Area Ratio (Std. Dev.)	Median Rising Edge Parameter (Std. Dev.)
Young Athletic	0.018 (0.001)	0.94 (0.15)	2.75 (0.29)
Young Non-Athletic	0.019 (0.003)	0.95 (0.26)	2.86 (0.56)
Old Healthy	0.014 (0.003)	0.51 (0.27)	1.95 (0.59)
Old Unhealthy	0.013 (0.002)	0.45 (0.18)	1.8 (0.38)

Table 8.1: Median Rising Slopes, Median Rising Edge Area Ratios, and Median Rising Edge Parameters by Cardiovascular Health Classification

	Median S-D Parameter (Std. Dev.)
Young Athletic	0.75 (0.3)
Young Non-Athletic	0.33 (0.22)
Old Healthy	0.03 (0.08)
Old Unhealthy	0.01 (0.13)

Table 8.2: Median S-D Parameters by Cardiovascular Health Classification

	Median PWA Score (Std. Dev.)
Young Athletic	3.51 (0.57)
Young Non-Athletic	3.19 (0.78)
Old Healthy	1.98 (0.66)
Old Unhealthy	1.81 (0.5)

Table 8.3: Median PWA Scores by Cardiovascular Health Classification

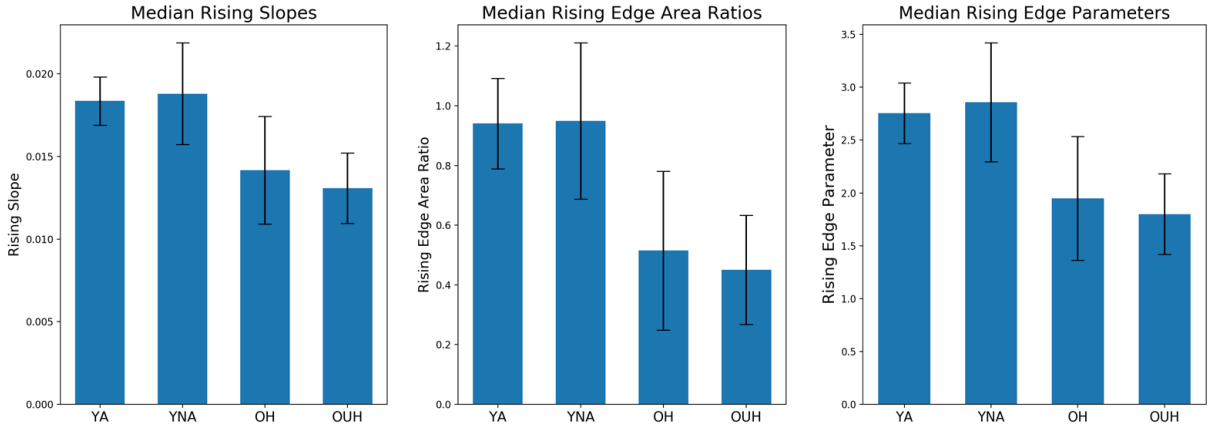

Figure 8.6: Median Rising Slopes, Rising Edge Area Ratios, and Rising Edge Parameters by Cardiovascular Health Classification

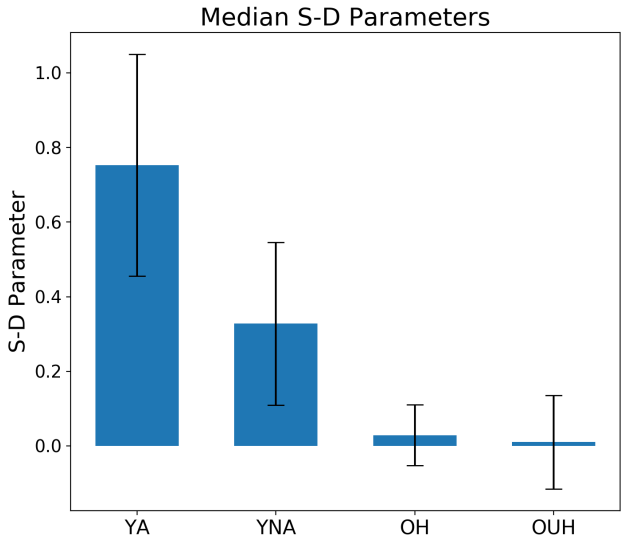

Figure 8.7: Median S-D Parameters by Cardiovascular Health Classification

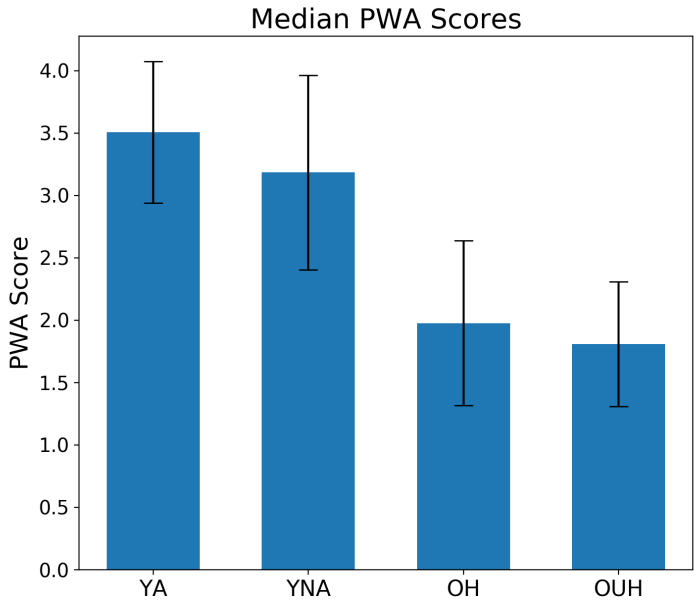

Figure 8.8: Median PWA Scores by Cardiovascular Health Classification

8.6 Discussion

Although there is a visual graphical difference in Figure 8.5 between the PPG waveforms of young athletic individuals and young non-athletic individuals, where athletic individuals typically all have visible undulations, it is difficult to establish a difference between old healthy individuals and old unhealthy individuals just by eye. This demonstrates the need to quantify features of the PPG waveforms in order to better assess the degree of atherosclerosis.

The results of these clinical studies show that our PWA Score is an effective quantification of PWA features, characterizing the rising edge and the falling edge of a PPG signal. The median PWA scores showed a decreasing trend with deteriorating cardiovascular health. It is important to note that using the rising edge features and the S-D parameter separately, we also see the same trend. In particular, the rising edge features better distinguished old healthy

people from old unhealthy people, whereas the S-D parameter was more useful for characterizing the difference between young athletic people and young non-athletic people. These results confirm our speculation that the S-D parameter is most useful in detecting the early stages of atherosclerosis, and the rising edge parameter is more useful in detecting the later stages of atherosclerosis.

Future work is needed to determine which features are actually the most useful in quantifying progression of atherosclerosis and arterial stiffness. For example, it may be better to use rising edge and S-D parameters separately, rather than summing them together as a composite PWA score due to the large variability in pulse waveforms. An individual could have a higher rising edge parameter, but a lower S-D parameter, and this would not be accurately reflected in their PWA score.

Through this study, we also found that proper techniques for measuring the PPG signal are necessary to obtain a good pulse reading that the algorithms are able to analyze. Factors such as hand stability and subject posture all impacted the PPG recordings. In the future, the mobile app could be improved to provide better visual feedback that a good steady pulse has been detected.

8.7 Conclusions

In this chapter, I described in detail two clinical studies on PWA features conducted at MIT and the Sengupta Hospital and Research Institute. By comparing average PPG waveforms of study subjects from four different cardiovascular health classifications, I validated the new PWA algorithms that I developed. Rising Edge Parameter, S-D Parameter, and PWA Score all demonstrated ability to characterize differences among the four different categories. The results

of these studies show promising potential in using these PWA features to assess the extent of atherosclerosis.

In the future, it would be useful to include these features as part of Botong Ma's machine learning algorithm for further evaluation to assess which features work the best, and their performance on large sets of data. In the next chapter, I describe our clinical study for PWV conducted in Nagpur, India and present the results.

Chapter 9

Clinical Study for Pulse Wave Velocity (PWV)

9.1 Study Objectives

In order to validate the NAJA device and better understand the distinction between healthy patients, at-risk patients, and CAD patients, we designed and conducted a clinical study in conjunction with the Sengupta Hospital and Research Institute located in Nagpur, India. This study was approved by both the MIT IRB committee, known as COUHES, under protocol number 1811598864, and by the IRB committee in Nagpur. The collected data was analyzed and used to train our machine learning model. This study protocol was initially designed by Niccolò Pignatelli, and has continued through multiple phases of data collection.

9.2 Study Population

As previously stated, study subjects were sorted into three groups: CAD patients, pre-CAD patients, and "healthy" subjects. The healthy subjects group consisted of 42 age-matched control subjects who did not have any of CAD, hypertension, or diabetes. These control subjects were recruited from family and friends of the hospital patients. The CAD patients group consisted of 26 cardiac patients who were clinically diagnosed with coronary arterial disease

(CAD), which was confirmed using CT scan calcium scoring and an echocardiogram. The pre-CAD patients group consisted of 32 cardiac patients who were not yet diagnosed with CAD, but possessed strong risk factors, specifically diabetes and/or hypertension.

We made an effort to recruitment patients of different ages. Specifically, each group had around the same number of patients that were age 55 or over and under age 55.

9.3 Study Protocol

Each subject in the study went through standard physical exam, where their blood pressure, height, weight, and various anthropometric distances were measured. Table 9.1 specifies the anthropometric measurements taken.

Anthropometric Measurements
Ear-Carotid
Carotid-Shoulder
Shoulder-Elbow
Elbow-Index Finger
Carotid-Groin
Groin-Knee
Knee-Ankle
Ankle-Toe

Table 9.1: Anthropometric Measurements Required for Calculating PWV

When performing the PWV measurement, subjects were asked to lie down on a hospital bed, so the PPG probes could be attached to the earlobe, index finger, and big toe as shown in Figure 9.1. With the NAJA device attached to the mobile phone, the mobile application was used in order to capture a 30 second recording of the PPG waveforms.

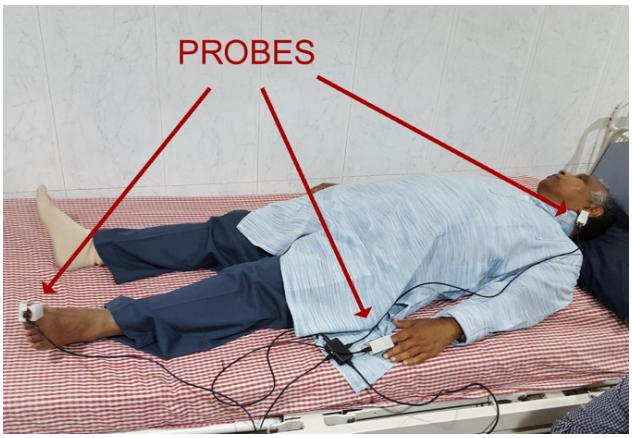

Figure 9.1: Study Subject Undergoing Multi-Site PPG Recording

9.4 Data Analysis

The raw data collected by the phone is saved as a time series CSV file containing ear, finger, and toe signals. To analyze the waveforms and determine PWV, we first pre-process the data by filtering. Figure 9.2 illustrates a noisy raw signals versus filtered signals. Then, the time delay between ear-toe peaks and ear-finger peaks is calculated to determine an average PTT_{ET} and PTT_{EF}. Using these values along with the anthropometric measurements in Table 9.1, we calculate PWV_{ET} and PWV_{EF}.

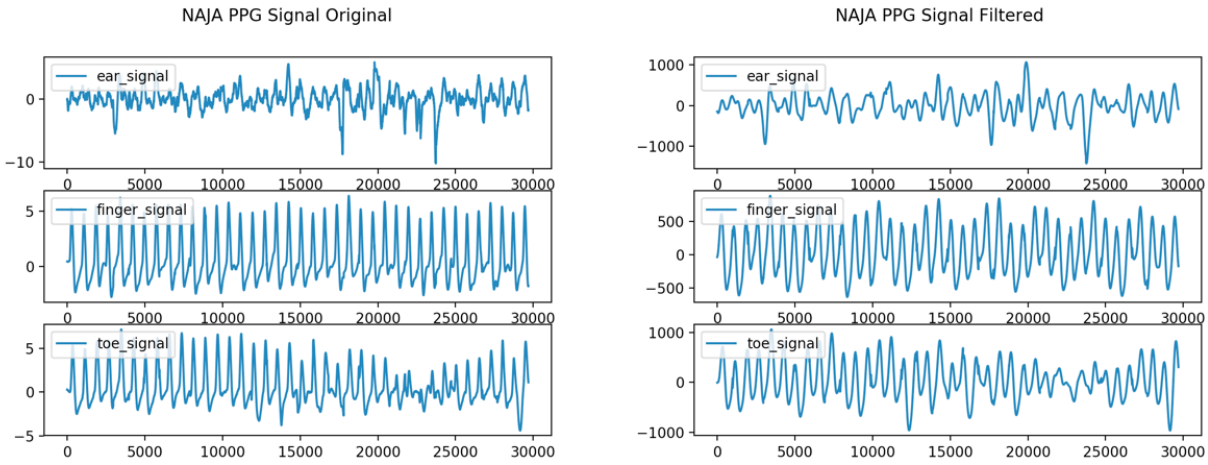

Figure 9.2: Noisy (left) vs Filtered (right) NAJA Ear, Finger, and Toe Signals

9.5 Results

The summary results for median PWV values are shown in Tables 9.2 and 9.3 and displayed as graphs in Figures 9.3 and 9.4. Because PWV increases as a non-linear function of age, a standard approach for analysis would be to derive a healthy baseline PWV as a function of age. With a limited number of patients however, the approach that we took was to stratify the data into two age groups: age under 55 and age 55 or above. The coarse stratification yields a larger variance in the PWV values, but is sufficient enough to support the trend of PWV as a function of age.

	Under 55 (Std. Dev.)	**Over 55 (Std. Dev.)**
Healthy	8.4 (1.5)	9.7 (1.3)
Pre-CAD	10.2 (1.2)	11.6 (1.8)
CAD	12.2 (1.0)	14.2 (1.4)

Table 9.2: Median PWV_{ET} Values

	Under 55 (Std. Dev.)	**Over 55 (Std. Dev.)**
Healthy	9.4 (2.0)	7.5 (1.5)
Pre-CAD	8.8 (1.9)	10.0 (1.6)
CAD	12.0 (1.1)	10.6 (1.7)

Table 9.3: Median PWV_{EF} Values

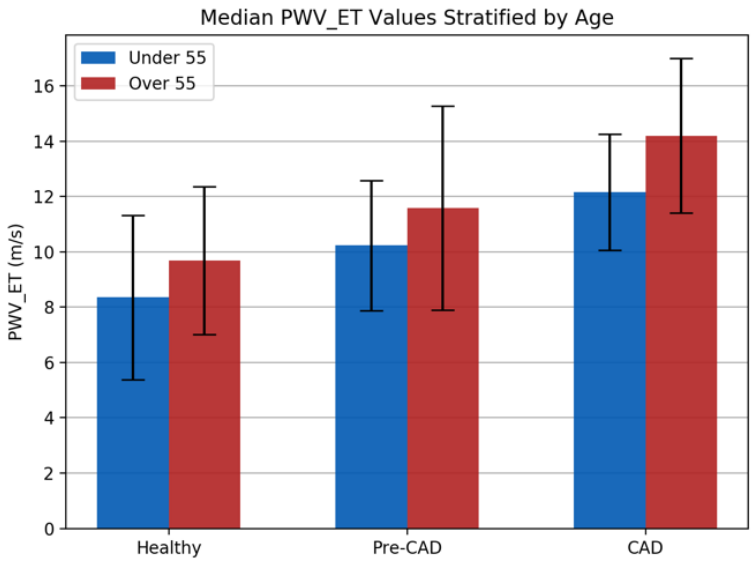

Figure 9.3: PWV Values Calculated from Ear-Toe(ET) Probe Signals

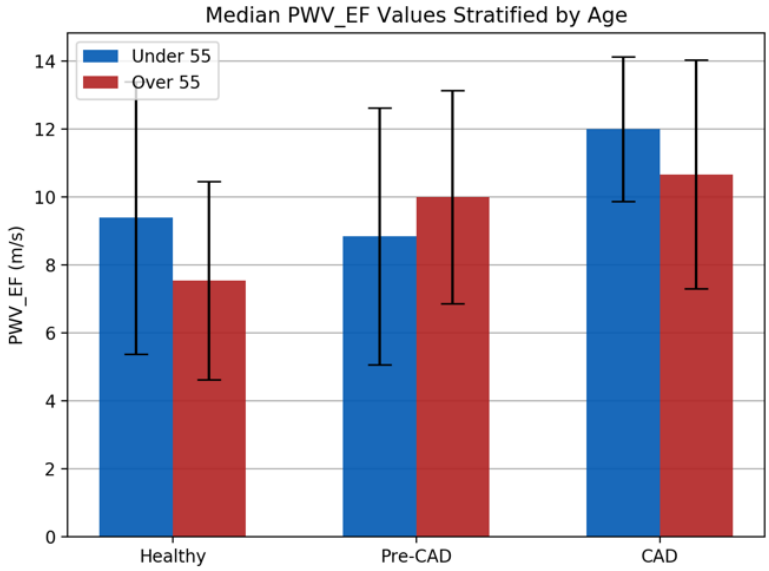

Figure 9.4: PWV Values Calculated from Ear-Finger(EF) Probe Signals

9.6 Machine Learning Analysis

To analyze our model, logistic regression was used to handle multi-dimensional data and display easily interpretable results. Rather than attempting to predict three separate classes, a binary classifier was used by combining the CAD and Pre-CAD groups to result in a classification of patients as “healthy” or “at-risk/unhealthy.” Considering our limited data size of

N=100, *k*-fold cross-validation was used to achieve a better estimate of the performance of the model.

During analysis, combinations of three simple features (Pulse Transit Time, patient height, and patient leg length) were tested, each of which could be easily measured in practice. The combination results were compared to the more extensive PWV calculation result. Summaries of the results in terms of the area under the curve (AUC) of the receiver operating curve (ROC) are found in Table 9.4 and Figure 9.5.

The feature combination with the best performance was PTT_{ET} and Height, with a mean AUC of 0.83, which was essentially equal to the performance of PWV_{ET}. An AUC value of 0.8 to 0.9 is considered excellent [56], and to demonstrate this comparatively, we also show that the use of the Ear-Finger pathway, PWV_{EF}, produces a very poor classifier, with AUC value< 0.6.

Feature Combinations	Mean AUC (Std. Dev.)
PWV_{ET}	0.81 (0.17)
PTT_{ET}, Height	0.83 (0.18)
PTT_{ET}, Leg Length	0.78 (0.25)
PWV_{EF}	0.51 (0.21)
PTT_{EF}, Height	0.50 (0.28)

Table 9.4: Mean AUC for Different Feature Combinations

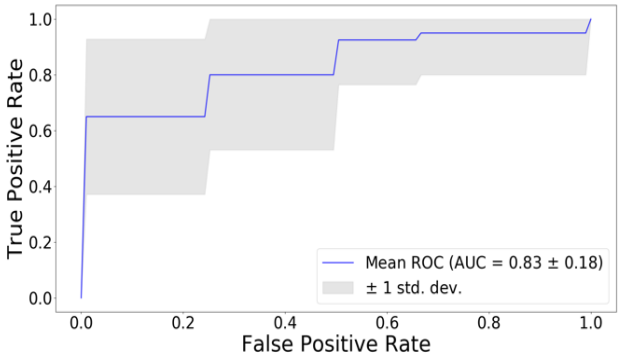

Figure 9.5: Cross Validation ROC Curve using PTT_{ET} and Height as Features

9.7 Discussion

Our study data showed that there was a strong increase in PWV with deteriorating cardiovascular health and increasing age. In general, PWV_{ET} values were higher than PWV_{EF} values. The Ear-Finger data, however, showed a significantly higher variability when compared with the Ear-Toe data, and also yielded some unexpected results. As seen in Figure 9.6, the median PWV_{EF} value was sometimes higher for the younger age group than the older age group.

We then used different feature combinations of PWV, PTT, patient height, and patient leg length to test our machine learning model. We found that using PTT_{ET} and height as features achieved comparable results to only using $PWV_{ET,}$ resulting in an AUC value of 0.83.

Through the clinical studies, we also found that the ear pulse is often very weak and difficult to find, especially in sick, elderly people. It was helpful to have professional medical staff around to help find the pulse. This further indicates that users of the NAJA device should undergo some basic training to be able to collect good pulse signals. Similar to the camera PPG app, it would also be helpful to include more visual feedback indicating that a steady pulse has been detected.

9.8 Conclusions

Results from our clinical study confirmed the previous notion that the PWV in the central artery behaves very differently from PWV in the peripheral muscular arteries. Because of this, we concluded that the muscular arteries were unreliable measurement sites for atherosclerosis and CAD assessments. The Ear-Toe measurement however, which included the central artery segment, yielded better results and was more effective for use as a screening tool.

While our study found the usefulness of the PWV_{ET} as an indicator of atherosclerosis and CAD, the pulse wave velocity calculation requires a number of different anthropometric measurements (Table 9.1). The collection of all these measurements can be too time-consuming and meticulous for a doctor or health worker that is busy. To address this issue, we conducted machine learning to see if we could come up with a CAD screening algorithm that uses a simpler set of measurements.

Machine learning analysis showed that only measuring the pulse timing, PTT_{ET}, and the patient height, would be enough to determine the risk of coronary arterial disease at a good accuracy rate (>80%). This result means that it may be possible to avoid taking certain anthropometric measurements altogether in a screening, which would reduce the time required and the potential for error caused by a variability in measurements.

Chapter 10

Summary and Conclusions

10.1 Summary of Work and Findings

In this thesis, I have successfully demonstrated two mobile screening tools to assess cardiovascular health. One tool is based on pulse wave analysis, and a more advanced tool based on pulse wave velocity.

The pulse wave analysis tool, which was implemented entirely on the mobile phone, made use of a few parameters: Rising Edge Parameter, S-D Parameter, and a composite PWA Score. These were calculated from the shape of the average pulse waveform. Based on a small study with 19 university students (9 athletic, 10 non-athletic), and a larger study with 35 older individuals (18 healthy, 17 unhealthy), this tool demonstrated sufficient sensitivity to distinguish between the different cardiovascular health categories. Young athletic individuals exhibited a median PWA Score of 3.51 (0.57), young non-athletic individuals exhibited a median PWA Score of 3.19 (0.78), old healthy individuals exhibited a median PWA Score of 1.98 (0.66), and old unhealthy individuals exhibited a median PWA Score of 1.81 (0.5).

The pulse wave velocity tool was implemented with external PPG hardware clips on a patient's ear, finger, and toe. The mobile phone simultaneously captures pulse recordings from

all three sites, and a separate algorithm calculates the pulse timings. Using certain anthropometric measurements, such as the patient's height and leg length, the pulse wave velocity can be calculated. Based on a clinical study with 100 patients (26 with coronary arterial disease, 32 at-risk, and 42 healthy), I improved our machine learning algorithms and demonstrated that the new algorithm is able to reliably distinguish healthy patients from non-healthy (CAD and at-risk) with an AUC of 0.83 (0.18).

The technology developed and refined in this thesis demonstrates that it is possible to create a low-cost mobile screening tool for CVD that can be implemented in a global health setting and used by health staff. For community health workers, a simple mobile phone pulse wave analysis tool can be used. For low-resource primary health clinics, which have beds available and a few medically trained staff, a more specific pulse wave velocity tool can be used.

10.2 Thesis Contributions

10.2.1 PWA Data Analysis Algorithms

Building on the previous work by Botong Ma, in this thesis, I have further developed the PWA data analysis algorithms. I have improved the rising edge parameter, and addressed the problem of not being able to quantify the falling edge of all types of PPG curves. I utilized corresponding areas from the second derivative and the original curve to create a composite PWA score capable of characterizing any arbitrary PPG curve. I also improved the peak finding algorithm used to extract individual peaks from the raw dataset by removing outlier peaks that could be due to noise or motion, and all unsmooth curves. Then, PWA scores were calculated for each of the remaining peaks, and the best four peaks were used to construct a canonical PPG peak. The canonical peak was then analyzed using PWA features including the Rising Edge

Parameter, S-D Parameter, and total PWA Score. These scoring metrics were validated in our clinical studies at MIT and the Sengupta Hospital and Research Institute.

10.2.2 PWV Data Analysis Algorithms

Building on the previous work done by Botong Ma, in this thesis I have further developed the PWV algorithm and improved the machine learning model. I improved the peak finding algorithm to throw out outlier peaks which are potentially due to noise or movement. I also automated the calculation of PWV, which was previously done manually using PTT and body measurements in Excel. Additionally, through our clinical study in Nagpur, India, I found that using PTT_{ET} and height as machine learning features, we were able to achieve comparable results to using PWV_{ET}. These promising results indicate that we do not need to take multiple body measurements, which can be both tedious and inaccurate, and simply measure height.

10.2.3 Android Mobile Phone Software

Given the previous challenges of needing to manually extract data from the mobile phones for analysis on a separate computer, I integrated the PWA and PWV mobile apps with a container app and the server. This design is better because the container app serves as a central hub for of our screening tools, and is able to run server analyses with a set of selected measurements. This would work well for organizing and efficiently analyzing large sets of data in real-time, and would encourage adoption of our mobile CVD screening toolkit in the real world.

10.2.4 Server Development

Using the generic server framework developed by John Mofor, I developed the custom APIs and database models for the CVD server to enable communication between the phone and server. I also integrated the existing pulse wave analysis and pulse wave velocity algorithms with the server to enable remove analysis of the patient data on the server. Having an integrated server platform is vital for the scalability and practicality of our CVD screening tools.

10.3 Future Work

With the contributions of this thesis, we now have an initial version of a practical platform that can be used in a real-world setting. Our group has several global health partners located in different countries, and we look forward to deploying these technologies as part of larger scale field tests. These technologies have great potential to have a positive impact in global health and help address the serious burden of cardiovascular disease throughout the world.

Bibliography

[1] Saladin K, *Anatomy & Physiology: The Unity of Form and Function*. 8th ed. Boston, MA: McGraw-Hill; 2001.

[2] Baig M, Smart Monitoring Systems for Alert Generation During Anaesthesia. Master's thesis. Auckland University of Technology, 2010.

[3] Weinhaus A J, Roberts K P, Anatomy of the Human Heart. In: Iaizzo P, ed. *Handbook of Cardiac Anatomy, Physiology, and Devices.* Totowa, NJ: Humana Press, Inc.; 2005:51-79.

[4] Lilly L, *Pathophysiology of Heart Disease: A Collaborative Project of Medical Students and Faculty.* 6th ed. Wolters Kluwer; 2016.

[5] Ma B, Developing a Low-Cost Cardiovascular Mobile Screening Kit. Master's thesis. *Massachusetts Institute of Technology*. 2019.

[6] World Health Organization. Cardiovascular Diseases, 2020. Accessed 2020-01-18.

[7] Smith SC Jr, Collins A, Ferrari R, et al. Our time: a call to save preventable deaths from cardiovascular disease (heart disease and stroke). *Circulation*. 2012;126:2769 –2775.

[8] Ritchie H, Roser M. Causes of Death. *OurWorldInData.org.* 2020. Accessed 2020-01-18.

[9] World Heart Federation. Different heart diseases, 2017. Accessed 2020-01-18.

[10] Yusef S, Hawken S, Ounpuu S, et al. Effect of potentially modifiable risk factors associated with myocardial infarction in 52 countries (the INTERHEART study): case-control study. *Lancet.* 2004; 364:937–952.

[11] Global atlas on cardiovascular disease prevention and control: policies, strategies and interventions. Mendis S, Puska P, Norrving B, ed. Geneva, Switzerland: World Health Organization; 2011.

[12] Global health risks: mortality and burden of disease attributable to selected major risks. Geneva, Switzerland: World Health Organization; 2009.

[13] Franklin B, Brinks J, Friedman H. Foundational factors for cardiovascular disease: behavioral change as a first-line preventive strategy. *Professional Heart Daily.* American Heart Association; 2013.

[14] InformedHealth.org [Internet]. Cologne, Germany: Institute for Quality and Efficiency in Health Care (IQWiG); 2006-. Coronary artery disease: Overview. 2013 Feb 13 [Updated 2017 Jul 27]. Available from: https://www.ncbi.nlm.nih.gov/books/NBK355313/

[15] National Heart, Lung, and Blood Institute. Atherosclerosis. Accessed 2020-01-18. Retrieved from https://www.nhlbi.nih.gov/health-topics/atherosclerosis

[16] Ruf M, Morgan O, Mackenzie K. Differences between Screening and Diagnostic Tests and Case Finding. *Health Knowledge*. Public Health Action Support Team. Accessed 2020-01-18. Retrieved from www.healthknowledge.org.uk/public-health-textbook

[17] Chokshi M, Patil B, Khanna R, et al. Health systems in India. *Journal of perinatology : official journal of the California Perinatal Association*. 2016;*36*(s3):S9–S12.

[18] Mahmood SS, Levy D, Vasan RS, Wang TJ. The Framingham Heart Study and the epidemiology of cardiovascular disease: a historical perspective. *Lancet*. 2014;383(9921):999–1008.

[19] Wilson P, Agostino R, Levy D, et al. Prediction of coronary heart disease using risk factor categories. *Circulation*. 1998;97:1837–1847.

[20] Global atlas on cardiovascular disease prevention and control: policies, strategies and interventions. Mendis S, Puska P, Norrving B, ed. Geneva, Switzerland: World Health Organization; 2011.

[21] Hippisley-Cox J, Coupland C, Vinogradova Y, et al. Derivation and validation of QRISK, a new cardiovascular disease risk score for the United Kingdom: prospective open cohort study. *BMJ*. 2007;335:136.

[22] Cook NR, Paynter NP, Eaton CB, et al. Comparison of the Framingham and Reynolds Risk Scores for global cardiovascular risk prediction in the multiethnic women's health initiative. *Circulation.* 2012;125:1748-1756.

[23] Beevers G, Lip GY, O'Brien E. ABC of hypertension. Blood pressure measurement. Part I-sphygmomanometry: factors common to all techniques. *BMJ*. 2001;322(7292):981–985.

[24] Li KHC, White FA, Tipoe T, et al. The current state of mobile phone apps for monitoring heart rate, heart rate variability, and atrial fibrillation: narrative review. *JMIR Mhealth Uhealth*. 2019;7(2):e11606.

[25] Kurylyak Y, Lamonaca F, Grimaldi D. Smartphone-Based Photoplethysmogram Measurement. In: Duro R, Lopez-Pena F. ed. *Digital Image, Signal and Data Processing for Measurement Systems.* River Publishers; 2012:135-164.

[26] Martinez-Perez B, de la Torre-Diez I, Lopez-Coronado M, et al. Mobile apps in cardiology: review. *JMIR Mhealth Uhealth*. 2013;1(2):e15.

[27] Asada HH, Shaltis P, Reisner A, et al. Mobile monitoring with wearable photoplethysmographic biosensors. *IEEE Engineering in Medicine and Biology.* 2003;22(3):28-40.

[28] Pevnick JM, Birkeland K, Zimmer R, et al. Wearable technology for cardiology: an update and framework for the future. *Trends in Cardiovascular Medicine.* 2018;28(2):144-150.

[29] Pantelopoulos A, Bourbakis NG. A survey on wearable sensor-based systems for health monitoring and prognosis. *IEEE Transactions on Systems Man and Cybernetics Part C (Applications and Reviews).* 2010;40(1):1-12.

[30] Plante TB, Urrea B, MacFarlane ZT, et al. Validation of the instant blood pressure smartphone app. *JAMA Internal Medicine.* 2016;176(5):700-702.

[31] Pignatelli N. Design of a mobile kit for cardiovascular disease screening in resource constrained environments. Master's thesis. *Massachusetts Institute of Technology*. 2017.

[32] Doupis J, Papanas N, Cohen A, et al. Pulse Wave Analysis by Applanation Tonometry for the Measurement of Arterial Stiffness. *The Open Cardiovascular Medicine Journal.* 2016;10:188–195.

[33] Mofor J. Pymedserver: A server framework for mobile data collection and machine learning. Master's thesis. *Massachusetts Institute of Technology*. 2019.

[34] Tamura Y, Maeda Y, Sekine M, Yoshida M. Wearable Photoplethysmographic Sensors—Past and Present. *Electronics*. 2014; 3(2):282-302.

[35] Gorczewska A. Influence of Sensor Design and Optical Properties of Tissue on the Photoplethysmographic Signal. *PhD Interdisciplinary Journal*. 2012.

[36] Elgendi M. On the Analysis of Fingertip Photoplethysmogram Signals. *Current Cardiology Reviews.* 2012; 8(1):14-25.

[37] Dawber T R, Thomas H E, McNamara P M. Characteristics of the dicrotic notch of the arterial pulse wave in coronary heart disease. *Angiology*. 1973; 24(4):244-55.

[38] Tigges T, Music Z, Pielmus A, et al. Classification of morphologic changes in photoplethysmographic waveforms. *Current Directions in Biomedical Engineering*. 2016; 2(1):203-207.

[39] Atly SR, Angarita-Jaimes N, Millaseau SC, et al. Predicting arterial stiffness from the digital volume pulse waveform. *IEEE Transactions on Biomedical Engineering*. 2007;54(12):2268-2275.

[40] Moxham IM. Understanding arterial pressure waveforms. *Southern African Journal of Anaesthesia and Analgesia.* 2003;9(1):40-42.

[41] Pereira T, Correia C, Cardoso J. Novel methods for pulse wave velocity measurement. *Journal of Medical and Biological Engineering.* 2015;35(5):555-565.

[42] O'Rourke MF, Staessen JA, Vlachopoulos C, et al. Clinical applications of arterial stiffness; definitions and reference values. *American Journal of Hypertension.* 2002;15:426-444.

[43] Butlin M, Qasem A. Large artery stiffness assessment using SphygmoCor technology. *Pulse (Basel)*. 2017;4(4):180-192.

[44] Calabia J, Torguet P, Garcia M, et al. Doppler ultrasound in the measurement of pulse wave velocity: agreement with the Complior method. *Cardiovascular Ultrasound.* 2011;9:13.

[45] E-nnovation biodiscovery Pvt. Ltd. SphygmoCor Xcel PWAPWV. Accessed: 2020-01-21.

[46] ALAM Medical. Complior Analyse. Accessed: 2020-01-21.

[47] Allen J, Murray A. Variability of photoplethysmography peripheral pulse measurements at the ears, thumbs, and toes. *IEE Proceedings – Science, Measurement and Technology.* 2000;147(6):403-407.

[48] Nitzan M, Romem A, Koppel R. Pulse oximetry: fundamentals and technology update. *Medical Devices (Auckland, N.Z.)*. 2014;7:231-239.

[49] Mitchell GF, Pulse wave velocity measuring device. 2001.

[50] Kortekaas MC, Niehof SP, van Velzen MHN, et al. Comparison of bilateral pulse arrival time before and after induced vasodilation by axillary block. *Physiological Measurement*. 2012;33(12):1993-2002.

[51] Chauhan S. A Mobile Platform for Non-invasive Diabetes Screening. Master's thesis. *Massachusetts Institute of Technology.* 2019.

[52] Django REST framework. Class-based views, 2020. Accessed: 2020-01-11.

[53] Django REST framework. Serializers, 2020. Accessed: 2020-01-11.

[54] Django. Models, 2020. Accessed: 2020-01-11.

[55] Django. Making queries, 2020. Accessed: 2020-01-11.

[56] Mandrekar JN. Receiver Operating Characteristic curve in diagnostic test assessment. *Journal of Thoracic Oncology.* 2010;5(9):1315-1316.